Human Rab GTPase- and class V myosin-dependent membrane tethering in a chemically defined reconstitution system

Motoki Inoshita[1], Joji Mima[1]*

[1]Institute for Protein Research, Osaka University, Suita, Osaka, Japan

***For correspondence:**
Joji Mima
Institute for Protein Research, Osaka University, 3-2 Yamadaoka, Suita, Osaka 565-0871, Japan
Tel.: +81 6 6879 4326
Fax: +81 6 6879 4329
E-mail: Joji.Mima@protein.osaka-u.ac.jp

Article style:

Research Article

Major subject areas:
Biochemistry, Cell Biology

Competing interests:
The authors have no competing interests to declare.

Funding:
The Ministry of Education, Culture, Sports, Science and Technology, Japan (MEXT) (to Joji Mima)

Abstract

Membrane tethering is a fundamental reaction to confer the specificity of membrane trafficking in eukaryotic cells. Although Rab-family GTPases and specific Rab-interacting effector proteins have been reported to be responsible for membrane tethering, whether and how these key components directly and specifically tether subcellular membranes still remain enigmatic. Using the chemically defined systems reconstituted with purified human Rabs and synthetic liposomes, we now establish that Rab-family GTPases have the conserved function to directly trigger membrane tethering, even in the absence of any types of Rab effectors. Furthermore, we strikingly demonstrate that membrane tethering mediated by endosomal Rab11a is selectively stimulated by the cognate Rab effectors, class V myosins, in a GTP-dependent manner. These findings postulate the novel concept that Rab proteins are a *bona fide* membrane tether to physically link two distinct lipid bilayers, and Rab effectors, including class V myosins, are rather a regulator of Rab-mediated membrane tethering.

Impact statement

Biochemical reconstitution studies reveal that human Rab GTPases are a *bona fide* membrane tether and class V myosin motors specifically promote membrane tethering mediated by their cognate Rab GTPase.

Introduction

All eukaryotic cells, from yeast to human cells, deliver the collect sets of the cargoes such as proteins and lipids to the appropriate cellular compartments including a variety of subcellular organelles, the plasma membrane, and the extracellular space (**Bonifacino and Glick, 2004**). These membrane trafficking events are a fundamental and highly selective process in the eukaryotic endomembrane systems, ensuring that transport vesicles or other membrane-bounded carriers specifically recognize, physically bind to, and eventually fuse with the target membranes in a spatiotemporally regulated manner (**Bonifacino and Glick, 2004**). A large body of prior genetic and biochemical studies have described miscellaneous key protein components functioning in eukaryotic membrane trafficking, which include SNAREs (soluble *N*-ethylmaleimide-sensitive factor attachment protein receptors) (**Jahn and Scheller, 2006**), SNARE-binding cofactors and chaperones such as Sec1/Munc18 proteins (**Baker and Hughson, 2016**), Rab-family small GTPases **(Stenmark, 2009**; **Hutagalung and Novick, 2011**), and Rab-interacting proteins termed "Rab effectors" (**Grosshans et al., 2006**; **Wandinger-Ness and Zerial, 2014**). Membrane tethering mediated by Rab GTPases and Rab effectors is generally known to be the first contact between the transport carriers and the target membranes and thus an essential step to determine the specificity of intracellular membrane trafficking (**Waters and Pfeffer, 1999**; **Cai et al., 2007**; **Yu and Hughson, 2010**), followed by SNARE-mediated membrane fusion, which is another critical layer to confer the fidelity of membrane trafficking (**Scales et al., 2000**; **McNew et al., 2000**; **Parlati et al., 2002**; **Izawa et al., 2012**; **Furukawa and Mima, 2014**). However, how Rab GTPases and Rab effectors work together to specifically drive membrane tethering has still remained elusive (**Brunet and Sacher, 2014**; **Tamura and Mima, 2014**), although recent biochemical reconstitution studies have begun to report the intrinsic membrane tethering potency of specific Rab effectors (**Yu and Hughson, 2010**; **Hickey and Wickner, 2010**; **Ho and Stroupe, 2015**; **Cheung et al., 2015**;

69 **Ho and Stroupe, 2016**; **Murray et al., 2016**) and Rab GTPases (**Lo et al., 2012**; **Tamura and Mima,**
70 **2014**). In this study, to gain a deeper insight into the mechanisms of intracellular membrane
71 tethering, we have reconstituted membrane tethering reactions in a chemically defined system
72 from synthetic liposomes and purified human Rab GTPases and class V myosins as the cognate
73 effectors of Rab11a, thereby comprehensively investigating their genuine functions in membrane
74 tethering.
75

Results and discussion

Prior two studies on membrane tethering in a chemically defined reconstitution system have described that tethering of synthetic liposomes can be directly triggered by several Rab-family GTPases themselves, which locate and function at the endosomal compartments in yeast (**Lo et al., 2012**) and human cells (**Tamura and Mima, 2014**). This Rab-mediated tethering of liposomal membranes is an efficient and specific biochemical reaction, as we established that membrane-anchored human Rab5a rapidly induced the formation of massive liposome clusters, and also that the tethering activity of Rab5a was able to be strictly and reversibly controlled by the membrane attachment and detachment of Rab proteins on both apposing membranes (**Tamura and Mima, 2014**). These our results strongly suggest the critical requirement of *trans*-Rab-Rab interactions on two distinct opposing membranes for a reversible membrane tethering event (**Tamura and Mima, 2014**).

In the current reconstitution study, to further comprehensively investigate the inherent membrane tethering potency of Rab-family GTPases in human, we purified and tested the six representative Rab GTPases functioning in the endocytic pathways (Rab4a, Rab5a, Rab7a, Rab9a, Rab11a, and Rab14) (**Wandinger-Ness and Zerial, 2014**), for typical non-endosomal Rabs, Rab1a in ER-to-Golgi traffic and Rab3a in exocytosis (**Stenmark, 2009**; **Hutagalung and Novick, 2011**), and also HRas for the control protein of a non-Rab small GTPase in the Ras superfamily (**Rojas et al., 2012**) (**Figure 1A**). All of the Rab-family and HRas GTPase proteins were purified as their full-length forms, consisting of the N-terminal non-conserved flexible segments (5-30 residues), the conserved globular Ras-superfamily GTPase domains in the middle (160-170 residues), and the so-called C-terminal hypervariable region (HVR) domains (20-50 residues) (**Rojas et al., 2012**) (**Figure 1A,B**; **Figure 1 – figure supplement 1**). In addition to the full-length amino acid sequences

of native proteins, to mimic membrane binding and anchoring of native Rab and HRas proteins through their isoprenyl or palmitoyl lipid anchors at the C-terminus (**Hutagalung and Novick, 2011**; **Rojas et al., 2012**), these recombinant Rab and HRas proteins used here were further artificially modified with a C-terminal polyhistidine tag (His12), which can be stably associated with synthetic liposomal membranes bearing a DOGS-NTA lipid (1,2-dioleoyl-sn-glycero-3-{[N-(5-amino-1-carboxypentyl)iminodiacetic acid]-succinyl}) (**Figure 1B**; **Figure 2A**). We employed GTPase activity assays for all of the purified Rab-His12 and HRas-His12 proteins, indicating that they retained the comparable intrinsic GTPase activities, which specifically converted GTP to GDP and a free phosphate (**Figure 1C**). Thus, this establishes that purified Rab-His12 and HRas-His12 proteins from the current preparations are all well folded and functionally active in solution (**Figure 1C**).

Dissecting the membrane tethering potency of human Rab GTPases in a chemically defined reconstitution system

The intrinsic potency of human Rab GTPases to directly drive membrane tethering was thoroughly evaluated by the kinetics of increase in turbidity of liposome suspensions in the presence of Rab proteins, which can be monitored by measuring the absorbance at 400 nm (**Figure 2**; **Figure 3**) (**Ohki et al., 1982**; **Hui et al., 2011**; **Tamura and Mima, 2014**; **Liu et al., 2015**). Rab-anchored liposomes were generated with purified Rab-His12 proteins and synthetic liposomes (400 nm in diameter) bearing a DOGS-NTA lipid and five major lipid species of phosphatidylcholine (PC), phosphatidylethanolamine (PE), phosphatidylinositol (PI), phosphatidylserine (PS), and cholesterol, roughly recapitulating lipid compositions of subcellular organelle membranes in mammalian cells (**Figure 2A**) (**van Meer et al., 2008**). With respect to Rab proteins tested in the tethering assays, as prior studies using the chemically defined reconstitution system had reported

the intrinsic tethering activity of several Rabs in the endocytic trafficking pathways of yeast (the Rab5 ortholog Vps21p) (**Lo et al., 2012**) and human cells (Rab5a and Rab7a) (**Tamura and Mima, 2014**), first we selected six representative endosomal Rabs (Rab4a, Rab5a, Rab7a, Rab9a, Rab11a, and Rab14) in human for comprehensively analyzing the tethering potency of Rab-family GTPases (Figure 2B-G). By applying the liposome turbidity assay to the six Rab proteins at variable concentrations, ranging from 0.5 μM to 4 μM towards 0.5 mM total lipids in the reactions (Figure 2A), rapid increase in liposome turbidity was triggered specifically either by Rab5a or Rab7a even at the low protein concentrations (0.5–1.0 μM, corresponding to the protein-to-lipid molar ratios of 1:1000–1:500) (Figure 2C,D). This establishes the very high potency of these two endosomal Rabs to directly catalyze membrane tethering reactions *in vitro*, consistent with our prior study on membrane tethering mediated by human Rabs (**Tamura and Mima, 2014**). Moreover, when assayed with the high protein concentrations of Rabs such as 4 μM (protein-to-lipid ratio, 1:125), we revealed that not only Rab5a and Rab7a (Figure 2C,D) but also all of the other endosomal Rabs (Rab4a, Rab9a, Rab11a, and Rab14) retained the significant intrinsic capacity to initiate efficient tethering of synthetic liposomes by themselves (Figure 2B,E,F,G). These data led us to propose the conserved function for all the endosomal Rab-family GTPases to physically link two distinct lipid bilayers together for membrane tethering events.

To what extent can the Rab protein densities on a membrane surface used in the current liposome turbidity assays (Figure 2) recapitulate the physiological conditions at subcellular membranes in mammalian cells? Using synaptic vesicles as a model of a trafficking organelle, previous comprehensive proteomic and lipidomic analyses of highly purified synaptic vesicles from rat brain determined the average copy numbers per vesicle of the major protein constituents including Rab-family GTPases (**Takamori et al., 2006**). Those quantitative data indicate that, on

148 average, approximately 10 copies of Rab3a and 15 copies of the other Rab GTPases, thus 25 copies
149 of Rab proteins in total are present in each single purified synaptic vesicle (**Takamori et al., 2006**).
150 Assuming (i) this copy number of synaptic Rabs (25 copies/vesicle), (ii) a mean outer diameter of
151 synaptic vesicles of 42 nm (**Takamori et al., 2006**), (iii) a typical bilayer thickness of 4 nm (**Nagle**
152 **and Tristram-Nagle, 2000**), and (iv) an average area occupied by a single phospholipid molecule
153 of 0.65 nm^2 (**Nagle and Tristram-Nagle, 2000**), we estimated the surface areas of the outer and
154 inner lipid layers of synaptic vesicles (5,540 nm^2 and 3,630 nm^2, respectively) that bore 14,100
155 lipid molecules in total, thereby giving approximately the Rab protein-to-lipid molar ratio of 1:560
156 (25 Rabs/vesicle, 14,100 lipids/vesicle). It should be noted that, in the current chemically defined
157 system, Rab5a and Rab7a (at least) can trigger rapid and efficient membrane tethering at the Rab-
158 to-lipid molar ratio of 1:500 (Figure 2C,D, black bold lines), which is almost identical to the
159 physiological ratio calculated above (Rab-to-lipid, 1:560). In addition to the Rab-to-lipid molar
160 ratios, we also quantitatively estimated the membrane surface areas occupied by Rab proteins in
161 the current reconstitution experiments (Figure 2). Assuming that (i) Rab proteins are typically a
162 spherical 25 kDa protein with an average radius of 2.0 nm (**Erickson, 2009**), (ii) all of the Rab-His12
163 molecules added to the reactions are stably attached to liposomal membranes containing a DOGS-
164 NTA lipid (Figure 2A), and (iii) a single 400-nm-diameter liposome contains 1,520,000 lipid
165 molecules (the total surface area, 985,000 nm^2; the surface area/lipid, 0.65 nm^2) (**Nagle and**
166 **Tristram-Nagle, 2000**), the percentages of the membrane surface coverage by Rab proteins were
167 calculated to be in the range of 3.79% to 30.3% (0.5 μM – 4.0 μM Rab proteins; the Rab-to-lipid
168 ratio, 1:1000 – 1:125) (Figure 2). These estimated values of the surface coverage by Rab proteins
169 reflect that Rab proteins occupy only a minor portion of the membrane surface areas of liposomes
170 in the turbidity assays and thus appear to have plenty of space to interact and cooperate with
171 other proteins and lipids on the membranes. Taken together, the Rab-to-lipid molar ratios and

membrane surface areas occupied by Rabs that we estimated above support the idea that endosomal Rab proteins can drive rapid and efficient membrane tethering *in vitro* under the physiological or physiologically relevant conditions mimicking subcellular membranes in mammalian cells.

Our data of the current liposome turbidity assays have revealed the conserved membrane tethering potency of endosomal Rab proteins in the context of a physiologically relevant function (Figure 2B-G). Next, we asked whether the intrinsic membrane tethering potency of human Rabs is the specialized function exclusively for Rab-family small GTPase proteins among the Ras superfamily GTPases (**Rojas et al., 2012**) and, moreover, for the Rab proteins that are specifically localized at the endosomal compartments. To address this, we performed the turbidity assays for the HRas protein as the model of a non-Rab Ras-superfamily GTPase (Figure 3A,B) and for two of the well-studied non-endosomal Rab proteins, Rab1a in ER-to-Golgi traffic and Rab3a in exocytosis (Figure 3A,C,D), with the same range of the protein concentrations as tested in Figure 2B-G (0.5 μM – 4.0 μM HRas or Rab proteins; the protein-to-lipid molar ratios, 1:1000 – 1:125). Indeed, HRas had little membrane tethering potency, giving no significant increase in the turbidity of liposomes when assayed even at the highest HRas protein concentrations of 4.0 μM (HRas-to-lipid, 1:125) (Figure 3B). Nevertheless, both of the non-endosomal Rab GTPases tested, Rab1a and Rab3a, retained the intrinsic capacity to directly induce efficient membrane tethering of synthetic liposomes (Figure 3C,D), as shown earlier with six endosomal Rabs in Figure 2. It should be noted that the difference of the *in vitro* membrane tethering potency between different Rab-family members and also between Rab proteins and HRas is not simply relied on their attachment to liposomal membranes in the tethering reactions (Figure 4). To examine the membrane association of Rab and HRas proteins in the current reconstitution systems, liposome co-sedimentation assays

196 were employed (Figure 4A) with the same experimental conditions as in the liposome turbidity
197 assays (Figure 2, Figure 3; protein-to-lipid, 1:500), demonstrating that all the tested Rab-family
198 and HRas proteins bound were able to comparably and stably bind to liposomal membranes
199 (Figure 4B,C,D,E,F,G,H,I,J). Thus, our data from the turbidity assays (Figure 2, Figure 3) suggest
200 that the intrinsic potency to physically tether two apposed membranes is selectively encoded in
201 the Rab-family members among the Ras-superfamily GTPases and likely to be fully conserved
202 through all the Rab-family members functioning in the endocytic and secretory pathways.
203
204 To further confirm the intrinsic membrane tethering capacity of Rab-family GTPases as their
205 genuine function, we employed fluorescence microscopic observations of the reconstituted
206 reactions of Rab-mediated membrane tethering (Figure 5). The tethering reactions were
207 incubated with rhodamine (Rh)-labeled fluorescent liposomes (0.5 mM lipids; 1000 nm diameter)
208 and Rab-family or HRas proteins (4 μM proteins; protein-to-lipid, 1:125) (Figure 5A) as in the
209 liposome turbidity assays (Figure 2; Figure 3). Strikingly, whereas only small particles of non-
210 tethered liposomes were observed when incubated in the absence of any Rab proteins (Figure
211 5B,C) or with the control HRas protein (Figure 5T,U), all of the tested endosomal and non-
212 endosomal Rab proteins (Rab4a, Rab5a, Rab7a, Rab9a, Rab11a, Rab14, Rab1a, and Rab3a) were
213 able to specifically induce the formation of substantial massive clusters of liposomes (Figure 5D-
214 S). Liposome clusters observed in the fluorescence images were then quantitatively analyzed for
215 the particle size distributions (Figure 6A), yielding the average sizes of Rab-mediated liposome
216 clusters ranging from 7.8 μm^2 to 55 μm^2, which are much larger than those of the control reactions
217 (0.92 μm^2 and 0.80 μm^2 for the reactions without any Rabs and with HRas, respectively) (Figure
218 6B). These our morphological analyses of Rab-mediated membrane tethering reactions by
219 fluorescence microscopy were fully consistent with the results obtained in the liposome turbidity

assays (Figure 2; Figure 3), thus further establishing the working model that Rab-family proteins themselves can be a *bona fide* membrane tether to directly and physically link two distinct lipid bilayers of subcellular membranes in intracellular membrane tethering.

Class V myosins, the Rab11a effectors, strongly and selectively promote membrane tethering mediated by the cognate Rab GTPase

By comprehensively and quantitatively characterizing *in vitro* membrane tethering reactions reconstituted with chemically defined lipid bilayers and purified recombinant proteins of eight Rab GTPases in human (Rab1a, Rab3a, Rab4a, Rab5a, Rab7a, Rab9a, Rab11a, and Rab14) (Figure 1; Figure 2; Figure 3; Figure 4; Figure 5; Figure 6), we now establish that Rab-family proteins genuinely have the intrinsic potency to directly and specifically tether two distinct lipid bilayers together in the context of a physiologically relevant function. Nevertheless, it is noteworthy that there appears to be wide variability in the tethering capacity of human Rab-family GTPases, although Rab proteins share the highly conserved amino acid sequences and tertiary structures for their Ras-superfamily GTPase domains (Figure 1A; Figure 1 – figure supplement 1) (**Rojas et al., 2012**; **Khan and Ménétrey, 2013**), which exhibited comparable GTP-hydrolysis activities for all the eight Rabs tested (Figure 1C). For typical instances of variability in the Rab-mediated tethering potency, Rab5a and Rab7a were able to trigger rapid membrane tethering at the protein-to-lipid molar ratios of 1:500 (Figure 2C,D, black bold lines), whereas most of the other Rabs (Rab1a, Rab4a, Rab9a, Rab11a, and Rab14) showed little or no tethering activity under the same conditions of the Rab density on the membrane surface (Rab-to-lipid, 1:500) (Figure 2B,E,F,G, black bold lines; Figure 3C, black bold lines). These results led us to hypothesize that (i) the intrinsic tethering activity of Rab proteins is negatively autoregulated in general, especially in the case of the Rabs that cause very slow and inefficient membrane tethering by themselves (Rab1a,

Rab4a, Rab9a, Rab11a, and Rab14) and thus (ii) specific Rab-interacting proteins (Rab effectors) drastically enhance the capacity of their cognate Rabs to drive membrane tethering. To test this hypothesis, we next attempted to reconstitute membrane tethering reactions with Rab11a, which had exhibited the lowest tethering potency among the eight Rabs tested in the earlier liposome turbidity assays (**Figure 2F**), and the cognate Rab11a effectors, class V myosin motor proteins (Myo5A and Myo5B) (**Figure 7**). Although any Rab11a effectors identified, except for the Exoc6/Sec15 exocyst subunit (**Zhang et al., 2004**; **Wu et al., 2005**; **Wu and Guo, 2015**), have never been proposed or reported to be directly involved in membrane tethering events (**Stenmark, 2009**; **Hutagalung and Novick, 2011**; **Wandinger-Ness and Zerial, 2014**), it has been thought that, as Rab effectors, class V myosins directly bind and cooperate with the cognate Rab11a on transport vesicles to regulate the specificity of membrane trafficking (**Lapierre et al., 2001**; **Hammer and Wu, 2002**; **Hammer and Sellers, 2012**; **Lindsay et al., 2013**).

To reconstitute the Rab11a- and class V myosin-dependent membrane tethering reaction in a chemically defined system, we purified the globular tail domains of class V myosin proteins (Myo5A-GTD and Myo5B-GTD) in human, which correspond to the C-terminal residues 1534-1855 of myosin 5a (Myo5A) and the residues 1526-1848 of myosin 5b (Myo5B) (**Figure 7A,B**). It should be noted that previous biochemical and structural studies indicated that these globular tail domains of Myo5A and Myo5B were necessary and sufficient for binding to Rab11a (**Figure 7A**) (**Roland et al., 2011**; **Lindsay et al., 2013**; **Pylypenko et al., 2013**; **Pylypenko et al., 2016**). Using purified Myo5A-GTD and Myo5B-GTD proteins (**Figure 7B**), we employed liposome turbidity assays to test whether class V myosin proteins have an effect on membrane tethering reactions mediated by the cognate Rab11a (**Figure 7C,D,E**). Strikingly, Rab11a-mediated tethering was strongly promoted by addition of an equimolar amount (1 μM) or a 2-fold molar excess (2 μM) of

Myo5A-GTD (Figure 7D) or Myo5B-GTD (Figure 7E) over Rab11a (1 μM; Rab-to-lipid ratio, 1:500), exhibiting much higher initial rates of the turbidity increase than those in the absence of Myo5-GTD proteins. Morphological changes of liposomes in the tethering reactions with Rab11a and Myo5-GTDs were also analyzed by fluorescence microscopy (Figure 7F,G,H,I,J,K), indicating that Rab11a and Myo5-GTD proteins synergistically and specifically induced the formation of massive clusters of liposomes (Figure 7J,K). Thus, the current results from these two independent assays in a chemically defined system uncover the novel function of class V myosins to directly support membrane tethering mediated by their cognate Rab11a GTPase.

Since class V myosins are recognized as Rab effectors that, in general, selectively interact with the GTP-bound from of Rab proteins (**Hammer and Sellers, 2012**), we next tested the guanine nucleotide dependence of Rab11a- and Myo5-GTD-mediated membrane tethering by employing the liposome turbidity assays (Figure 8A). Indeed, the addition of GTP (1 mM) drastically stimulated the synergistic action of Rab11a and Myo5A-GTD (Figure 8B, blue lines) or Myo5B-GTD (Figure 8C, blue lines) upon driving rapid membrane tethering, but the presence of GTP had no effect on the tethering reactions bearing either Rab11a or Myo5-GTD proteins alone (Figure 8B,C, black and red lines). This direct stimulation by GTP on Rab11a/Myo5-GTD-dependent membrane tethering was shown as a very specific effect when added the variable GTP concentrations ranging from 1 μM to 1 mM (Figure 8D,E) and assayed with the other guanine nucleotides, GDP and GTPγS (Figure 8F,G). Our data therefore reflect that Myo5-GTD proteins greatly enhance the tethering activity of Rab11a in a GTP-dependent manner, suggesting that the direct and stable interactions of Myo5-GTD proteins with membrane-bound Rab11a-GTP proteins are required for facilitating membrane tethering. To experimentally test the association of Myo5-GTD proteins with Rab11a proteins on liposomal membranes, liposome co-sedimentation assays were performed under the

typical conditions used for the turbidity assays in Figure 8 (Rab-to-lipid ratio, 1:500; Rab-to-Myo5-GTD ratio, 1:1; 1 mM GTP) (Figure 9A). However, we found that the amounts of Myo5A-GTD (Figure 9B, ppt) and Myo5B-GTD (Figure 9E, ppt) bound to and co-isolated with Rab11a-attached liposomes were comparable to those of the control reactions with protein-free liposomes in the absence of Rab11a-His12 (Figure 9C,F, ppt) or in the presence of untagged Rab11a lacking a His12 tag (Figure 9D,G, ppt). This indicates, unexpectedly, that the membrane association of Myo5-GTD proteins was not significantly promoted by the recruitment of Rab11a on a liposomal membrane surface. Considering that rapid and efficient Rab11a-mediated membrane tethering is definitely relied on the presence of Myo5-GTD proteins and GTP in the current reconstitution system (Figure 7; Figure 8), our results from the co-sedimentation assays (Figure 9) may imply that the transient interactions between Rab11a and Myo5-GTD proteins on a membrane surface are essential for cooperatively accelerating membrane tethering reactions.

Our current studies have uncovered the novel function of class V myosins to directly promote membrane tethering mediated by their cognate Rab11a GTPase in a GTP-dependent manner, by thoroughly characterizing reconstituted membrane tethering in the chemically defined systems with purified Rab11a and Myo5-GTD proteins (Figure 7; Figure 8; Figure 9). However, it could still be argued that Myo5-GTD proteins can non-physiologically induce tethering or aggregation of liposomal membranes coated by other non-cognate Rab-His12 proteins or even coated by any types of soluble proteins modified with a polyhistidine tag. In this context, to more strictly validate the specificity of Rab11a/Myo5-GTD-dependent membrane tethering, we further explored the liposome turbidity assays in the presence of Myo5-GTD proteins (Figure 10A), not only for the cognate Rab11a but also for the other four Rab proteins including Rab1a, Rab4a, Rab9a, and Rab14, which had shown relatively slow and inefficient membrane tethering by themselves,

similar to Rab11a (Figure 2; Figure 3). Although Rab11a and either Myo5A-GTD or Myo5B-GTD proteins synergistically triggered very rapid and efficient membrane tethering (Figure 10B,C, blue lines), fully consistent with the earlier results in Figure 8, these Myo5-GTD proteins indeed had only minor or little effect on the tethering potency of Rab1a, Rab4a, Rab9a, and Rab14 (Figure 10B,C, green, black, cyan, and red lines). Thus, our data faithfully reflect that both Myo5A-GTD and Myo5B-GTD recognize and act upon exclusively the cognate Rab11a at the membrane surface of lipid bilayers, thereby selectively activating Rab11a-mediated membrane tethering reactions. The current findings from reconstituted membrane tethering with purified Rab and Myo5-GTD proteins (Figure 7; Figure 8; Figure 9; Figure 10) provide new insights into how Rab GTPases on subcellular membranes (transport vesicles, organelle membranes, or the plasma membrane) and class V myosin motors on actin cytoskeletal tracks cooperate with each other to promote membrane tethering and how their functions synergistically contribute to the spatiotemporal specificity of membrane tethering and beyond.

Conclusions

Membrane tethering is one of the most critical and important processes to determine the specificity of membrane traffic in eukaryotic endomembrane systems, delivering the correct sets of cargoes (proteins, lipids, etc.) to the correct locations (organelles, the plasma membrane, the extracellular space, etc.) (**Waters and Pfeffer, 1999**). From a large body of prior studies using genetic, cell biological, biochemical, and structural biological approaches on this essential membrane tethering process, we generally recognize that a number of diverse but specific types of “Rab effectors” have been described as the so-called “tethering factors”, such as coiled-coil tethering proteins and multisubunit tethering complexes (**Yu and Hughson, 2010**; **Chia and Gleeson, 2014**; **Kuhlee et al., 2015**). However, for the most cases, it remains ambiguous indeed

whether these "tethering factors" identified are a *bona fide* membrane tether that physically links two distinct opposing membranes by itself or, furthermore, whether they are even involved directly in membrane tethering events (**Brunet and Sacher, 2014**). In this context, in order to thoroughly define and characterize the molecular functions in membrane tethering for Rab-family GTPases and class V myosin cytoskeletal motor proteins as the specific Rab effectors, we have undertaken to recapitulate the membrane tethering machinery in the chemically defined systems reconstituted with synthetic lipid bilayers of liposomes and purified proteins of human Rab GTPases and class V myosins (**Figure 1**; **Figure 2**; **Figure 7**).

Our current *in vitro* reconstitution studies present three new findings supporting the working model of intracellular membrane tethering mediated by Rab-family GTPases as a genuine membrane tether: (1) All the eight Rab proteins tested, including both endosomal and non-endosomal Rabs, have the intrinsic capacity to physically tether two apposed membranes under the experimental conditions mimicking the lipid composition and Rab density of subcellular organelles/vesicles in mammalian cells, establishing the conserved tethering function of the Rab-family members (**Figure 2**; **Figure 3**; **Figure 5**). (2) The tethering capacity of Rab proteins is a specific function among the Ras superfamily GTPases and yet highly variable for each of different Rab proteins (**Figure 2**; **Figure 3**; **Figure 5**). This suggests that the Rab subfamily-specific (RabSF) motifs could be the regions responsible for controlling the membrane tethering potency of each Rab (**Pereira-Leal and Seabra, 2000**; **Stein et al., 2012**). Finally, (3) the Rab effectors, class V myosins, can drastically and specifically promote membrane tethering mediated by their cognate Rab GTPase, Rab11a, in a GTP-dependent manner (**Figure 7**; **Figure 8**; **Figure 10**). This finding leads us to hypothesize that cytoskeletal motor proteins, including class V myosins and also microtubule-based motor proteins, act as "tethering factors" (not "tethers") that directly and

364 positively regulate Rab-mediated membrane tethering (**Hammer and Wu, 2002**; **Akhmanova and**
365 **Hammer, 2010**). Understanding a detailed picture of the protein machinery of Rab-mediated
366 membrane tethering will need further studies using a chemically defined reconstitution system,
367 which may focus on testing tethering by the heterotypic Rab combinations, determining the
368 specific regions in Rab molecules responsible for tethering, and reconstituting Rab-mediated
369 tethering in the presence of different types of Rab effectors.
370

Materials and methods

Protein expression and purification

The coding sequences for the eight isoforms of Rab-family GTPases (Rab1a, Rab3a, Rab4a, Rab5a, Rab7a, Rab9a, Rab11a, and Rab14) in human and for human HRas GTPase were amplified by polymerase chain reaction (PCR) with Human Universal QUICK-Clone cDNA II (Clontech, Mountain View, CA) as a template cDNA and KOD-Plus-Neo DNA polymerase (Toyobo, Osaka, Japan), as described (**Tamura and Mima, 2014**). The amplified PCR fragments contained the sequence encoding a human rhinovirus (HRV) 3C protease site (Leu-Glu-Val-Leu-Phe-Gln-Gly-Pro) upstream of the initial ATG codons and the sequence encoding polyhistidine residues (His12) downstream of the codons for a C-terminal residue, yielding the full-length Rab and HRas proteins with three extra N-terminal residues (Gly-Pro-Gly) and a C-terminal His12 tag after HRV 3C protease cleavage. For Rab11a, the PCR fragment without the polyhistidine-coding sequence was also amplified as above, to prepare the Rab11a protein lacking the C-terminal His12 tag (untagged Rab11a). All of these PCR fragments for the Rab-family and HRas GTPases were inserted into a pET-41 Ek/LIC vector (Novagen, Madison, WI), which is designed to express an N-terminal GST-His6-tagged protein, by the ligation-independent cloning method (Novagen).

Recombinant Rab and HRas proteins were expressed in the *Escherichia coli* BL21(DE3) cells (Novagen) harboring the pET-41-based vectors in Lysogeny Broth (LB) medium (1 liter each) with kanamycin (50 μg/ml) by induction with 0.1 mM IPTG at 37°C for 3 hours. *E. coli* cells harvested after IPTG induction were resuspended in 40 ml each of RB150 (20 mM Hepes-NaOH, pH 7.4, 150 mM NaCl, 10% glycerol) containing 0.1 mM GTP, 5mM $MgCl_2$, 1 mM DTT, 1 mM PMSF, and 1.0 μg/ml pepstatin A, freeze-thawed in a liquid nitrogen and a water bath at 30°C, lysed by sonication using UD-201 ultrasonic disrupter (Tomy Seiko, Tokyo, Japan), and then ultracentrifuged at 50,000

395 rpm for 75 min at 4°C with a 70 Ti rotor (Beckman Coulter, Indianapolis, IN). The supernatants
396 obtained were mixed with COSMOGEL GST-Accept beads (50% slurry, 4 ml each; Nacalai Tesque,
397 Kyoto, Japan) and were incubated at 4°C for 2 hours with gentle agitation to isolate GST-His6-
398 tagged Rab-His12 and HRas-His12 proteins. The protein-bound GST-Accept beads were washed
399 four times in RB150 containing 5 mM $MgCl_2$ and 1 mM DTT (8 ml each), resuspended in the same
400 buffer (4 ml each), supplemented with HRV 3C protease (4 units/ml final; Novagen), and incubated
401 without agitation (4°C, 16 hours) to cleave off and elute Rab-His12 and HRas-His12 proteins. After
402 centrifugation of the bead suspensions (15,300 g, 10 min, 4°C), purified Rab-His12 and HRas-His12
403 proteins were harvested from the supernatants.
404
405 For class V myosins, the coding sequences of the globular tail domains of human myosin 5a
406 (Myo5A-GTD; residues 1534-1855) and myosin 5b (Myo5B-GTD; residues 1526-1848) with the
407 sequence encoding a HRV 3C-protease site upstream of the initial codons were amplified by PCR
408 as above and then cloned into a pET-30 Ek/LIC vector (Novagen) expressing an N-terminal His6-
409 tagged protein. Recombinant Myo5A-GTD (1534-1855) and Myo5B-GTD (1526-1848) proteins
410 were expressed in the *E. coli* BL21(DE3) cells harboring the pET-30-based vectors in LB medium
411 with kanamycin (1 liter each) by induction with 0.1 mM IPTG (16°C, 16 hours). *E. coli* cells were
412 resuspended in 40 ml each of RB150 containing $MgCl_2$ (5 mM), DTT (1 mM), PMSF (1 mM), and
413 pepstatin A (1.0 μg/ml), followed by freeze-thaw treatment, sonication, and ultracentrifugation as
414 above. The supernatants were mixed with Complete His-Tag Purification Resin beads (50% slurry,
415 4 ml each; Roche, Basel, Switzerland) and were incubated at 4°C for 2 hours with gentle agitation
416 to isolate His6-tagged Myo5A-GTD and Myo5B-GTD proteins. The protein-bound beads were
417 washed four times in RB150 containing 5 mM $MgCl_2$, 1 mM DTT, and 20 mM imidazole (8 ml each),
418 resuspended in the same buffer (2 ml each) containing HRV 3C protease (15 units/ml; Novagen),

and incubated with gentle agitation (4°C, 16 hours). After centrifugation of the bead suspensions (15,300 g, 10 min, 4°C), purified Myo5A-GTD and Myo5B-GTD proteins, which had been cleaved off from the beads, were harvested from the supernatants and dialyzed against RB150 containing 5 mM $MgCl_2$ and 1 mM DTT.

GTPase activity assay

GTP-hydrolysis activities of human Rab-family and HRas GTPases were assayed by quantitating released free phosphate molecules during the hydrolytic reactions, using the Malachite Green-based reagent Biomol Green (Enzo Life Sciences, Farmingdale, NY) as described (**Tamura and Mima, 2014**; **Sugiura and Mima, 2016**), with modifications. Purified recombinant Rab-family and HRas proteins (2 μM final) were incubated at 30°C for 1 hour in RB150 containing 6 mM $MgCl_2$, 1 mM DTT, and 1 mM GTP or GTPγS. After a 1-hour incubation, the reaction mixtures (50 μl each) were supplemented with the Biomol Green reagent (50 μl each), further incubated at 30°C for 30 min, and measured for absorbance at 620 nm in a clear 96-well microplate (Falcon no. 351172; Corning, Corning, NY) using the SpectraMax Paradigm plate reader with the ABS-MONO cartridge (Molecular Devices, Sunnyvale, CA). All of the data obtained were corrected by subtracting the absorbance values of the control reactions without any Rab and HRas GTPases. To calculate the concentrations of released phosphate molecules in the reactions, phosphate standard samples (2.5 – 160 μM final; Enzo Life Sciences) were also incubated and assayed using the same protocol. Means and standard deviations of the specific GTPase activities for purified Rab-family and HRas proteins (μM phosphate/min/μM protein) were determined from three independent experiments.

Liposome preparation

All of the non-fluorescent lipids were purchased from Avanti Polar Lipids (Alabaster, AL).

443 Fluorescent lipids, Rh-PE and FL-PE, were obtained from Molecular Probes (Eugene, OR). Lipid
444 mixes for the Rh-labeled liposomes used in liposome turbidity assays, fluorescence microscopy,
445 and liposome co-sedimentation assays contained 1-palmitoyl-2-oleoyl-PC (POPC) [42% (mol/mol)],
446 POPE (16.5%), soy PI (10%), POPS (5%), cholesterol (20%), DOGS-NTA (6%), and Rh-PE (0.5%).
447 Dried lipid films harboring the physiological mimic lipid composition (**van Meer et al., 2008**;
448 **Tamura and Mima, 2014**) were completely resuspended in RB150 containing 5 mM $MgCl_2$ and 1
449 mM DTT by vortexing, yielding 8 mM total lipids in final, then incubated at 37°C for 1 hour with
450 shaking, freeze-thawed in liquid N_2 and a water bath at 30°C, and extruded 21 times through
451 polycarbonate filters (pore diameter, 400 or 1000 nm; Avanti Polar Lipids) in a mini-extruder
452 (Avanti Polar Lipids) at 40°C. Lipid concentrations of the extruded liposomes were determined
453 from the fluorescence of Rh-PE (λex = 550 nm, λem = 590 nm) and FL-PE (λex = 486 nm, λem =
454 529 nm) using the SpectraMax Paradigm plate reader with the TUNE cartridge (Molecular Devices)
455 and a black 384-well plate (Corning no. 3676; Corning). Liposome solutions were diluted with
456 RB150 containing 5 mM $MgCl_2$ and 1 mM DTT to 5 mM total lipids in final and stored at 4°C.
457
458 **Liposome turbidity assay**
459 Membrane tethering of Rab GTPase-anchored liposomes was monitored by turbidity changes of
460 liposome solutions as described (**Ohki et al., 1982**; **Hui et al., 2011**; **Tamura and Mima, 2014**; **Liu**
461 **et al., 2015**), with modifications. After preincubating liposome suspensions and Rab protein
462 solutions separately at 30°C for 10 min, liposomes (400 nm diameter; 0.5 mM total lipids in final)
463 were mixed with Rab proteins (0.5 – 4.0 μM in final) in RB150 containing 5 mM $MgCl_2$ and 1 mM
464 DTT (total 150 μl for each), immediately followed by measuring the absorbance changes of the
465 liposome suspensions at 400 nm in a DU720 spectrophotometer (Beckman Coulter) at room
466 temperature for 300 sec. For the assays with class V myosins, Rab proteins (1 μM final) were

467 preincubated at 30°C for 30 min in the presence of Myo5A-GTD or Myo5B-GTD (0.5 – 2.0 μM final)
468 before mixing with liposomes. All liposome turbidity data were obtained from one experiment
469 and were typical of those from more than three independent experiments.
470
471 **Liposome co-sedimentation assay**
472 Rh-labeled liposome suspensions (400 nm diameter; 1 mM total lipids in final) were mixed with
473 purified Rab, HRas, or BSA proteins (2 μM in final) in RB150 containing 5 mM $MgCl_2$ and 1 mM DTT
474 (100 μl each) and subsequently incubated at 30°C for 30 min. For the experiments with class V
475 myosins, the reaction mixtures were further supplemented with GTP (1 mM final) and Myo5A-
476 GTD or Myo5B-GTD (2 μM final). After incubation, these reactions were ultracentrifuged at 50,000
477 rpm for 30 min at 4°C with a TLA100 rotor and an Optima TLX ultracentrifuge (Beckman Coulter).
478 The pellets and supernatants obtained were analyzed by SDS-PAGE and Coomassie Blue staining.
479
480 **Fluorescence microscopy**
481 After separately preincubating liposome suspensions and Rab protein solutions at 30°C for 10 or
482 30 min, liposomes (1000 nm diameter; 0.5 or 0.8 mM total lipids in final) and Rab proteins (3.0 or
483 4.0 μM final) were mixed in RB150 containing 5 mM $MgCl_2$ and 1 mM DTT (total 50 μl for each),
484 further incubated at 30°C for 30 min or 1 hour, transferred to ice, and subjected to fluorescence
485 microscopy. For the reactions with class V myosins, Rab11a-His12 (3 μM final) was preincubated
486 in the presence of Myo5A-GTD or Myo5B-GTD (3 μM final) at 30°C for 30 min before incubating
487 with liposomes. A drop of the incubated reactions (5 μl each) was placed on a microscope slide
488 (S2111; Matsunami Glass, Kishiwada, Japan) and covered with an 18-mm coverslip (Matsunami
489 Glass). Fluorescence microscopy was performed using a BZ-9000 fluorescence microscope
490 (Keyence, Osaka, Japan) equipped with Plan Apo 40X NA 0.95 and Plan Apo VC 100X NA 1.40 oil

491 objective lenses (Nikon, Tokyo, Japan) and TRITC and GFP-BP filters (Keyence). Digital images
492 obtained were processed using the BZ-II viewer application (Keyence) and the ImageJ2 software
493 (National Institutes of Health, Bethesda, MD). Particle sizes of Rab-mediated liposome clusters
494 were measured using ImageJ2 after setting the lower intensity threshold level to 100 and the
495 upper intensity threshold level to 255 (**Stroupe et al., 2009**; **Hickey and Wickner, 2010**).
496

Acknowledgements

We thank Dr. Naoki Tamura (Institute for Protein Research, Osaka University; now Fukushima Medical University School of Medicine) for valuable suggestions on this project and for substantial contributions to preparing the expression vectors for human Rab GTPases. We are grateful to Drs. Junichi Takagi and Yukiko Matsunaga (Institute for Protein Research, Osaka University) for access to fluorescence microscopy experiments. This study was in part supported by the Program to Disseminate Tenure Tracking System from the Ministry of Education, Culture, Sports, Science and Technology, Japan (MEXT) and Grants-in-Aid for Scientific Research from MEXT (to JM).

Author contributions

JM designed the research; JM and MI performed the experiments; JM and MI analyzed the data; JM wrote the manuscript.

References

Akhmanova A, Hammer JA 3rd. 2010. Linking molecular motors to membrane cargo. *Current Opinion in Cell Biology* **22**:479-487.
doi: 10.1016/j.ceb.2010.04.008

Baker RW, Hughson FM. 2016. Chaperoning SNARE assembly and disassembly. *Nature Reviews Molecular Cell Biology* **17**:465-479.
doi: 10.1038/nrm.2016.65

Bonifacino JS, Glick BS. 2004. The mechanisms of vesicle budding and fusion. *Cell* **116**:153-166.
doi: 10.1016/S0092-8674(03)01079-1

Brunet S, Sacher M. 2014. Are all multisubunit tethering complexes bona fide tethers? *Traffic* **15**:1282-1287.
doi: 10.1111/tra.12200

Cai H, Reinisch K, Ferro-Novick S. 2007. Coats, tethers, Rabs, and SNAREs work together to mediate the intracellular destination of a transport vesicle. *Developmental Cell* **12**:671-682.
doi: 10.1016/j.devcel.2007.04.005

Cheung PY, Limouse C, Mabuchi H, Pfeffer SR. 2015. Protein flexibility is required for vesicle tethering at the Golgi. *eLife* **4**:e12790.
doi: 10.7554/eLife.12790

Chia PZ, Gleeson PA. 2014. Membrane tethering. *F1000Prime Reports* **6**:74.
doi: 10.12703/P6-74

Erickson HP. 2009. Size and shape of protein molecules at the nanometer level determined by sedimentation, gel filtration, and electron microscopy. *Biological Procedures Online* **11**:32-51.
doi: 10.1007/s12575-009-9008-x

Furukawa N, Mima J. 2014. Multiple and distinct strategies of yeast SNAREs to confer the specificity of membrane fusion. *Scientific Reports* **4**:4277.
doi: 10.1038/srep04277

Grosshans BL, Ortiz D, Novick P. 2006. Rabs and their effectors: achieving specificity in membrane traffic. *Proceedings of the National Academy of Sciences of USA* **103**:11821-11827.
doi: 10.1073/pnas.0601617103

Hammer JA 3rd, Sellers JR. 2012. Walking to work: roles for class V myosins as cargo transporters. *Nature Reviews Molecular Cell Biology* **13**:13-26.
doi: 10.1038/nrm3248

Hammer JA 3rd, Wu XS. 2002. Rabs grab motors: defining the connections between Rab GTPases and motor proteins. *Current Opinion in Cell Biology* **14**:69-75.
doi: 10.1016/S0955-0674(01)00296-4

Hickey CM, Wickner W. 2010. HOPS initiates vacuole docking by tethering membranes before trans-SNARE complex assembly. *Molecular Biology of the Cell* **21**:2297-2305.
doi: 10.1091/mbc.E10-01-0044

Ho R, Stroupe C. 2015. The HOPS/class C Vps complex tethers membranes by binding to one Rab GTPase in each apposed membrane. *Molecular Biology of the Cell* **26**:2655-2663.
doi: 10.1091/mbc.E14-04-0922

Ho R, Stroupe C. 2016. The HOPS/class C Vps complex tethers high-curvature membranes via a direct protein-membrane interaction. *Traffic* **17**:1078-1090.
doi: 10.1111/tra.12421

Hui E, Gaffaney JD, Wang Z, Johnson CP, Evans CS, Chapman ER. 2011. Mechanism and function of synaptotagmin-mediated membrane apposition. *Nature Structural & Molecular Biology* **18**:813-821.
doi: 10.1038/nsmb.2075

Hutagalung AH, Novick PJ. 2011. Role of Rab GTPases in membrane traffic and cell physiology. *Physiological Reviews* **91**:119-149.
doi: 10.1152/physrev.00059.2009

Izawa R, Onoue T, Furukawa N, Mima J. 2012. Distinct contributions of vacuolar Qabc- and R-SNARE proteins to membrane fusion specificity. *The Journal of Biological Chemistry* **287**:3445-3453.
doi: 10.1074/jbc.M111.307439

Jahn R, Scheller RH. 2006. SNAREs--engines for membrane fusion. *Nature Reviews Molecular Cell Biology* **7**:631-643.
doi: 10.1038/nrm2002

Khan AR, Ménétrey J. 2013. Structural biology of Arf and Rab GTPases' effector recruitment and specificity. *Structure* **21**:1284-1297.
doi: 10.1016/j.str.2013.06.016

Kuhlee A, Raunser S, Ungermann C. 2015. Functional homologies in vesicle tethering. *FEBS Letters* **589**:2487-2497.
doi: 10.1016/j.febslet.2015.06.001

Lapierre LA, Kumar R, Hales CM, Navarre J, Bhartur SG, Burnette JO, Provance DW Jr, Mercer JA, Bähler M, Goldenring JR. 2001. Myosin Vb is associated with plasma membrane recycling systems. *Molecular Biology of the Cell* **12**:1843-1857.
doi: 10.1091/mbc.12.6.1843

Lindsay AJ, Jollivet F, Horgan CP, Khan AR, Raposo G, McCaffrey MW, Goud B. 2013. Identification and characterization of multiple novel Rab-myosin Va interactions. *Molecular Biology of the Cell* **24**:3420-3434.
doi: 10.1091/mbc.E13-05-0236

Liu TY, Bian X, Romano FB, Shemesh T, Rapoport TA, Hu J. 2015. Cis and trans interactions between atlastin molecules during membrane fusion. *Proceedings of the National Academy of Sciences of USA* **112**:E1851-E1860.
doi: 10.1073/pnas.1504368112

Lo SY, Brett CL, Plemel RL, Vignali M, Fields S, Gonen T, Merz AJ. 2012. Intrinsic tethering activity of endosomal Rab proteins. *Nature Structural & Molecular Biology* **19**:40-47.
doi: 10.1038/nsmb.2162

McNew JA, Parlati F, Fukuda R, Johnston RJ, Paz K, Paumet F, Söllner TH, Rothman JE. 2000. Compartmental specificity of cellular membrane fusion encoded in SNARE proteins. *Nature* **407**:153-159.
doi: 10.1038/35025000

Murray DH, Jahnel M, Lauer J, Avellaneda MJ, Brouilly N, Cezanne A, Morales-Navarrete H, Perini ED, Ferguson C, Lupas AN, Kalaidzidis Y, Parton RG, Grill SW, Zerial M. 2016. An endosomal tether undergoes an entropic collapse to bring vesicles together. *Nature* **537**:107-111.
doi: 10.1038/nature19326

Nagle JF, Tristram-Nagle S. 2000. Structure of lipid bilayers. *Biochimica et Biophysica Acta* **1469**:159-195.
doi: 10.1016/S0304-4157(00)00016-2

Ohki S, Düzgüneş N, Leonards K. 1982. Phospholipid vesicle aggregation: effect of monovalent and divalent ions. *Biochemistry* **21**:2127-2133.
doi: 10.1021/bi00538a022

Parlati F, Varlamov O, Paz K, McNew JA, Hurtado D, Söllner TH, Rothman JE. 2002. Distinct SNARE complexes mediating membrane fusion in Golgi transport based on combinatorial specificity. *Proceedings of the National Academy of Sciences of USA* **99**:5424-5429.
doi: 10.1073/pnas.082100899

Pereira-Leal JB, Seabra MC. 2000. The mammalian Rab family of small GTPases: definition of family and subfamily sequence motifs suggests a mechanism for functional specificity in the Ras superfamily. *Journal of Molecular Biology* **301**:1077-1087.
doi: 10.1006/jmbi.2000.4010

Pylypenko O, Attanda W, Gauquelin C, Lahmani M, Coulibaly D, Baron B, Hoos S, Titus MA, England P, Houdusse AM. 2013. Structural basis of myosin V Rab GTPase-dependent cargo recognition. *Proceedings of the National Academy of Sciences of USA* **110**:20443-20448.
doi: 10.1073/pnas.1314329110

Pylypenko O, Welz T, Tittel J, Kollmar M, Chardon F, Malherbe G, Weiss S, Michel CI, Samol-Wolf A, Grasskamp AT, Hume A, Goud B, Baron B, England P, Titus MA, Schwille P, Weidemann T, Houdusse A, Kerkhoff E. 2016. Coordinated recruitment of Spir actin nucleators and myosin V motors to Rab11 vesicle membranes. *eLife* **5**:e17523.
doi: 10.7554/eLife.17523

Rojas AM, Fuentes G, Rausell A, Valencia A. 2012. The Ras protein superfamily: evolutionary tree and role of conserved amino acids. *The Journal of Cell Biology* **196**:189-201. doi: 10.1083/jcb.201103008

Roland JT, Bryant DM, Datta A, Itzen A, Mostov KE, Goldenring JR. 2011. Rab GTPase-Myo5B complexes control membrane recycling and epithelial polarization. *Proceedings of the National Academy of Sciences of USA* **108**:2789-2794. doi: 10.1073/pnas.1010754108

Scales SJ, Chen YA, Yoo BY, Patel SM, Doung YC, Scheller RH. 2000. SNAREs contribute to the specificity of membrane fusion. *Neuron* **26**:457-464. doi: 10.1016/S0896-6273(00)81177-0

Stein M, Pilli M, Bernauer S, Habermann BH, Zerial M, Wade RC. 2012. The interaction properties of the human Rab GTPase family--comparative analysis reveals determinants of molecular binding selectivity. *PLoS One* **7**:e34870. doi: 10.1371/journal.pone.0034870

Stenmark H. 2009. Rab GTPases as coordinators of vesicle traffic. *Nature Reviews Molecular Cell Biology* **10**:513-525. doi: 10.1038/nrm2728

Stroupe C, Hickey CM, Mima J, Burfeind AS, Wickner W. 2009. Minimal membrane docking requirements revealed by reconstitution of Rab GTPase-dependent membrane fusion from purified components. *Proceedings of the National Academy of Sciences of USA* **106**:17626-17633. doi: 10.1073/pnas.0903801106

Sugiura S, Mima J. 2016. Physiological lipid composition is vital for homotypic ER membrane fusion mediated by the dynamin-related GTPase Sey1p. *Scientific Reports* **6**:20407. doi: 10.1038/srep20407

Takamori S, Holt M, Stenius K, Lemke EA, Grønborg M, Riedel D, Urlaub H, Schenck S, Brügger B, Ringler P, Müller SA, Rammner B, Gräter F, Hub JS, De Groot BL, Mieskes G, Moriyama Y, Klingauf J, Grubmüller H, Heuser J, Wieland F, Jahn R. 2006. Molecular anatomy of a trafficking organelle. *Cell* **127**:831-846. doi: 10.1016/j.cell.2006.10.030

Tamura N, Mima J. 2014. Membrane-anchored human Rab GTPases directly mediate membrane tethering *in vitro*. *Biology Open* **3**:1108-1115. doi: 10.1242/bio.20149340

van Meer G, Voelker DR, Feigenson GW. 2008. Membrane lipids: where they are and how they behave. *Nature Reviews Molecular Cell Biology* **9**:112-124. doi: 10.1038/nrm2330

Wandinger-Ness A, Zerial M. 2014. Rab proteins and the compartmentalization of the endosomal system. *Cold Spring Harbor Perspectives in Biology* **6**:a022616.

700 doi: 10.1101/cshperspect.a022616
701
702 **Waters MG**, Pfeffer SR. 1999. Membrane tethering in intracellular transport. *Current Opinion in*
703 *Cell Biology* **11**:453-459.
704 doi:10.1016/S0955-0674(99)80065-9
705
706 **Wu B**, Guo W. 2015. The exocyst at a glance. *Journal of Cell Science* **128**:2957-2964.
707 doi: 10.1242/jcs.156398
708
709 **Wu S**, Mehta SQ, Pichaud F, Bellen HJ, Quiocho FA. 2005. Sec15 interacts with Rab11 via a novel
710 domain and affects Rab11 localization in vivo. *Nature Structural Molecular Biology* **12**:879-885.
711 doi: 10.1038/nsmb987
712
713 **Yu IM**, Hughson FM. 2010. Tethering factors as organizers of intracellular vesicular traffic. *Annual*
714 *Review of Cell and Developmental Biology* **26**:137-156.
715 doi: 10.1146/annurev.cellbio.042308.113327
716
717 **Zhang XM**, Ellis S, Sriratana A, Mitchell CA, Rowe T. 2004. Sec15 is an effector for the Rab11 GTPase
718 in mammalian cells. *The Journal of Biological Chemistry* **279**:43027-43034.
719 doi: 10.1074/jbc.M402264200
720

Figure legends

Figure 1. Purification of human Rab GTPases used in this reconstitution study.

(**A**) Schematic representation of the endosomal Rabs (Rab4a, Rab5a, Rab7a, Rab9a, Rab11a, and Rab14), non-endosomal Rabs (Rab1a and Rab3a), and HRas GTPase in human, showing their amino acid residues, domains (Ras-superfamily GTPase domains and hypervariable regions), and intracellular locations, which include early endosome (EE), recycling endosome (RE), plasma membrane (PM), late endosome (LE), lysosome (Ly), endoplasmic reticulum (ER), Golgi, and secretory vesicle (SV).

(**B**) Coomassie Blue-stained gels of purified recombinant proteins of the C-terminally His12-tagged endosomal Rab, non-endosomal Rab, and HRas GTPases and the untagged form of Rab11a used in this study.

(**C**) Intrinsic GTP-hydrolysis activities of purified Rab proteins. Purified Rab-His12, HRas-His12, and untagged Rab11a proteins (2 μM) were incubated at 30°C for 1 h in RB150 containing $MgCl_2$ (6 mM), DTT (1 mM), and GTP (1 mM) or GTPγS (1 mM) for the control, followed by assaying released free phosphate molecules using a Malachite Green-based reagent.

Figure 1 – figure supplement 1. Amino acid sequence alignment of the Rab- and Ras-family GTPases in human used in this study. Multiple alignment of the sequences was performed using Clustal W (http://www.genome.jp/tools/clustalw/) and ESPript 3.0 (http://espript.ibcp.fr/ESPript/ESPript/).

Figure 2. Endosomal Rab GTPases directly initiate membrane tethering by themselves in a chemically defined reconstitution system.

(**A**) Schematic representation of liposome turbidity assays for testing Rab-mediated liposome

745 tethering in **B**-**G**.

746 (**B**-**G**) Endosomal Rab-His12 proteins (0.5 – 4 μM each), Rab4a-His12 (**B**), Rab5a-His12 (**C**), Rab7a-
747 His12 (**D**), Rab9a-His12 (**E**), Rab11a-His12 (**F**), and Rab14-His12 (**G**), were incubated with synthetic
748 liposomes bearing physiological mimic lipid composition (400 nm diameter; 0.5 mM lipids) in
749 RB150 containing $MgCl_2$ (5 mM) and DTT (1 mM) at room temperature for 300 sec. During
750 incubation, turbidity changes of the Rab-liposome mixed reactions were monitored by measuring
751 the absorbance at 400 nm. The protein-to-lipid molar ratios used for these turbidity reactions
752 were from 1:1000 to 1:125, as indicated.

753

754 **Figure 3.** Non-endosomal Rab GTPases have the inherent potency to specifically mediate
755 membrane tethering.
756 (**A**) Schematic representation of liposome turbidity assays for the non-Rab Ras superfamily GTPase,
757 HRas, and non-endosomal Rab GTPases, Rab1a in ER-Golgi traffic and Rab3a in exocytosis, in **B**-**D**.
758 (**B**-**D**) Liposome turbidity assays were employed as in Figure 2B-G, with HRas-His12 (**B**), Rab1a-
759 His12 (**C**), and Rab3a-His12 (**D**) proteins (0.5 – 4 μM each in final) and physiological mimic synthetic
760 liposomes (0.5 mM total lipids in final). The protein-to-lipid molar ratios used were indicated.

761

762 **Figure 4.** Membrane association of Rab-His12 proteins onto DOGS-NTA-bearing liposomes.
763 (**A**) Schematic representation of liposome co-sedimentation assays for testing membrane
764 attachment of Rab-His12 proteins used in Figure 2 and Figure 3.
765 (**B**-**K**) Rh-labeled liposomes (400 nm diameter; 1 mM total lipids in final) were incubated (30°C, 30
766 min) with Rab4a-His12 (**B**), Rab5a-His12 (**C**), Rab7a-His12 (**D**), Rab9a-His12(**E**), Rab11a-His12 (**F**),
767 Rab14-His12 (**G**), Rab1a-His12 (**H**), Rab3a-His12 (**I**), HRas-His12 (**J**), and BSA for a negative control
768 (**K**) (2 μM final for each), and ultracentrifuged (50,000 rpm, 30 min, 4°C). The supernatants (sup)

769 and precipitates (ppt) obtained were analyzed by SDS-PAGE and Coomassie Blue staining.

770

771 **Figure 5.** Rab-mediated membrane tethering induces the formation of massive liposome clusters.

772 (**A**) Schematic representation of fluorescence microscopic observations of Rab-mediated liposome

773 clusters.

774 (**B**-**U**) Fluorescence images (**B**, **D**, **F**, **H**, **J**, **L**, **N**, **P**, **R**, **T**) and bright field images (**C**, **E**, **G**, **I**, **K**, **M**, **O**, **Q**,

775 **S**, **U**) of Rab-mediated liposome clusters. Fluorescently-labeled liposomes bearing Rh-PE (1000

776 nm diameter; 0.5 mM lipids in final) were incubated at 30°C for 1 h, in the absence (**B**, **C**) and

777 presence of the Rab- and Ras-family GTPases (4 μM each in final), including Rab4a-His12 (**D**, **E**),

778 Rab5a-His12 (**F**, **G**), Rab7a-His12 (**H**, **I**), Rab9a-His12 (**J**, **K**), Rab11a-His12 (**L**, **M**), Rab14-His12 (**N**,

779 **O**), Rab1a-His12 (**P**, **Q**), Rab3a-His12 (**R**, **S**), and HRas-His12 (**T**, **U**), and subjected to fluorescence

780 microscopy. Scale bars: 20 μm.

781

782 **Figure 6.** Particle size distributions of liposome clusters induced by Rab-mediated membrane

783 tethering.

784 (**A**) Particle sizes of the Rab-mediated liposome clusters observed in the fluorescence images of

785 Figure 5.

786 (**B**) Particle numbers and average sizes of the Rab-mediated liposome clusters observed in the

787 fluorescence images of Figure 5.

788

789 **Figure 7.** Class V myosin globular tail domains, Myo5A-GTD and Myo5B-GTD, strongly stimulate

790 Rab11a-dependent membrane tethering.

791 (**A**) Schematic representation of class V myosins in human, Myo5A and Myo5B, showing their

792 amino acid residues and domains including myosin motor domains, IQ motifs, coiled coil regions,

and globular tail domains (GTDs). Representative Myo5-interacting Rab GTPases and the Rab-binding regions in Myo5A and Myo5B are indicated.

(**B**) The Coomassie Blue-stained gel of purified Myo5A-GTD and Myo5B-GTD proteins, which are comprised of the amino acid residues 1534-1855 and 1526-1848, respectively.

(**C**) Schematic representation of liposome turbidity assays for testing Rab11a- and Myo5-GTD-dependent liposome tethering in **D**, **E**.

(**D**, **E**) Liposome turbidity assays were employed with Rab11a-His12 (1 μM final) as in Figure 2F, but in the presence of Myo5A-GTD (**D**) and Myo5B-GTD (**E**) (0.5 – 2 μM final).

(**F**-**K**) Fluorescence images of Rab11a-mediated liposome clusters in the presence of Myo5-GTDs. Rab11a-His12 (3 μM final) and Myo5A-GTD or Myo5B-GTD (3 μM final) were preincubated at 30°C for 30 min, mixed with Rh-labeled liposomes (1000 nm diameter; 0.8 mM lipids in final), further incubated (30°C, 30 min), and subjected to fluorescence microscopy (**J**, **K**). For a control, Rab11a-His12, Myo5-GTD, or both were omitted from the reactions where indicated (**F**-**I**). Scale bars: 20 μm.

Figure 8. Guanine nucleotide dependence of Rab11a-mediated membrane tethering in the presence of Myo5A-GTD and Myo5B-GTD.

(**A**) Schematic representation of liposome turbidity assays for testing Rab11a- and Myo5-GTD-dependent liposome tethering in the presence of GTP in **B**-**G**.

(**B**, **C**) Rab11a/Myo5-dependent membrane tethering is strongly and specifically promoted by the addition of GTP. Liposome turbidity assays with Rab11a-His12 (1 μM) and Myo5A-GTD (1 μM) (**B**) or Myo5B-GTD (2 μM) (**C**) were performed as in Figure 7D, E, but in the presence of GTP (1 mM).

(**D**, **E**) Liposome turbidity assays were employed with Rab11a-His12 and Myo5A-GTD (**D**) or Myo5B-GTD (**E**) as in **B**, **C**, in the presence of various concentrations of GTP (1 μM – 1 mM).

817 (**F**, **G**) Liposome turbidity assays were employed with Rab11a-His12 and Myo5A-GTD (**F**) or Myo5B-
818 GTD (**G**) as in **B**, **C**, in the presence of GTP, GTPγS, and GDP (1 mM for each).
819
820 **Figure 9.** Membrane association of Myo5-GTD proteins onto Rab11a-anchored liposomes.
821 (**A**) Schematic representation of liposome co-sedimentation assays for testing membrane binding
822 of Myo5A-GTD and Myo5B-GTD to Rab11a-bound liposomes.
823 (**B**-**G**) Liposome co-sedimentation assays were employed as in Figure 4, with Rh-labeled liposomes
824 (400 nm diameter; 1 mM lipids) and Rab11a-His12 (2 μM) (**B**, **E**), but in the presence of Myo5A-
825 GTD (2 μM) (**B-D**), Myo5B-GTD (2 μM) (**E-G**), and GTP (1 mM). For a control, the reactions without
826 Rab11a-His12 (**C**, **F**) or with the untagged form of Rab11a lacking a His12 tag (untagged Rab11a)
827 (**D**, **G**) were also tested. The supernatants (sup) and precipitates (ppt) obtained were analyzed by
828 SDS-PAGE and Coomassie Blue staining.
829
830 **Figure 10.** Myo5A-GTD and Myo5B-GTD selectively activate Rab11a-dependent membrane
831 tethering.
832 (**A**) Schematic representation of liposome turbidity assays in **B**, **C**, for the various Rab GTPases
833 (Rab11a, Rab1a, Rab4a, Rab9a, and Rab14) in the presence of Myo5-GTDs and GTP.
834 (**B**, **C**) Myo5-GTDs specifically promote efficient membrane tethering mediated by the cognate Rab
835 GTPase, Rab11a. Liposome turbidity assays were employed with Myo5A-GTD (**B**) or Myo5B-GTD
836 (**C**) and GTP, as in Figure 8B, C, but for Rab11a, Rab1a, Rab4a, Rab9a, and Rab14 GTPases.
837

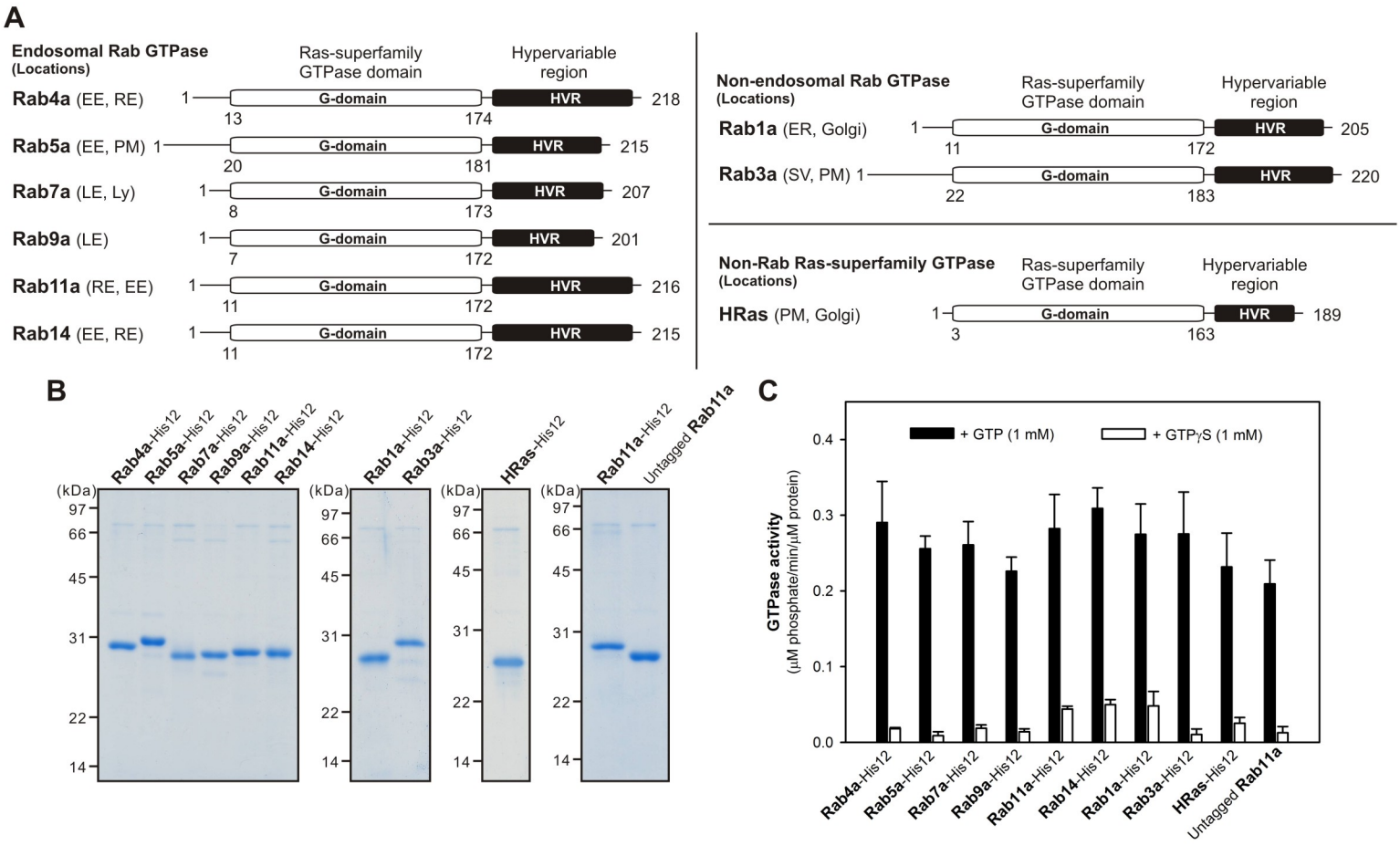

Figure 1. Purification of human Rab GTPases used in this reconstitution study.

（A) Schematic representation of theendosomal Rabs (Rab4a, Rab5a, Rab7a, Rab9a, Rab11a, and Rab14), non-endosomal Rabs (Rab1a and Rab3a), and HRas GTPase in human, showing their amino acid residues, domains (Ras-superfamily GTPase domains and hypervariable regions), andintracellular locations, which include early endosome (EE), recycling endosome (RE), plasma membrane (PM), late endosome (LE), lysosome (Ly), endoplasmic reticulum (ER), Golgi, and secretory vesicle (SV).

（B) Coomassie Blue-stained gels ofpurified recombinant proteins of the C-terminally His12-tagged endosomal Rab, non-endosomal Rab, and HRas GTPases and the untagged form of Rab11a used in this study.

（C) Intrinsic GTP-hydrolysis activities of purified Rab proteins. Purified Rab-His12, HRas-His12, and untagged Rab11a proteins (2 μM) were incubated at 30°C for 1 h in RB150 containing MgCl2 (6 mM), DTT (1 mM), and GTP (1 mM) or GTPγS (1 mM) for the control, followed by assaying released free phosphate molecules using a Malachite Green-based reagent.

Figure 1 - figure supplement 1. Inoshita & Mima

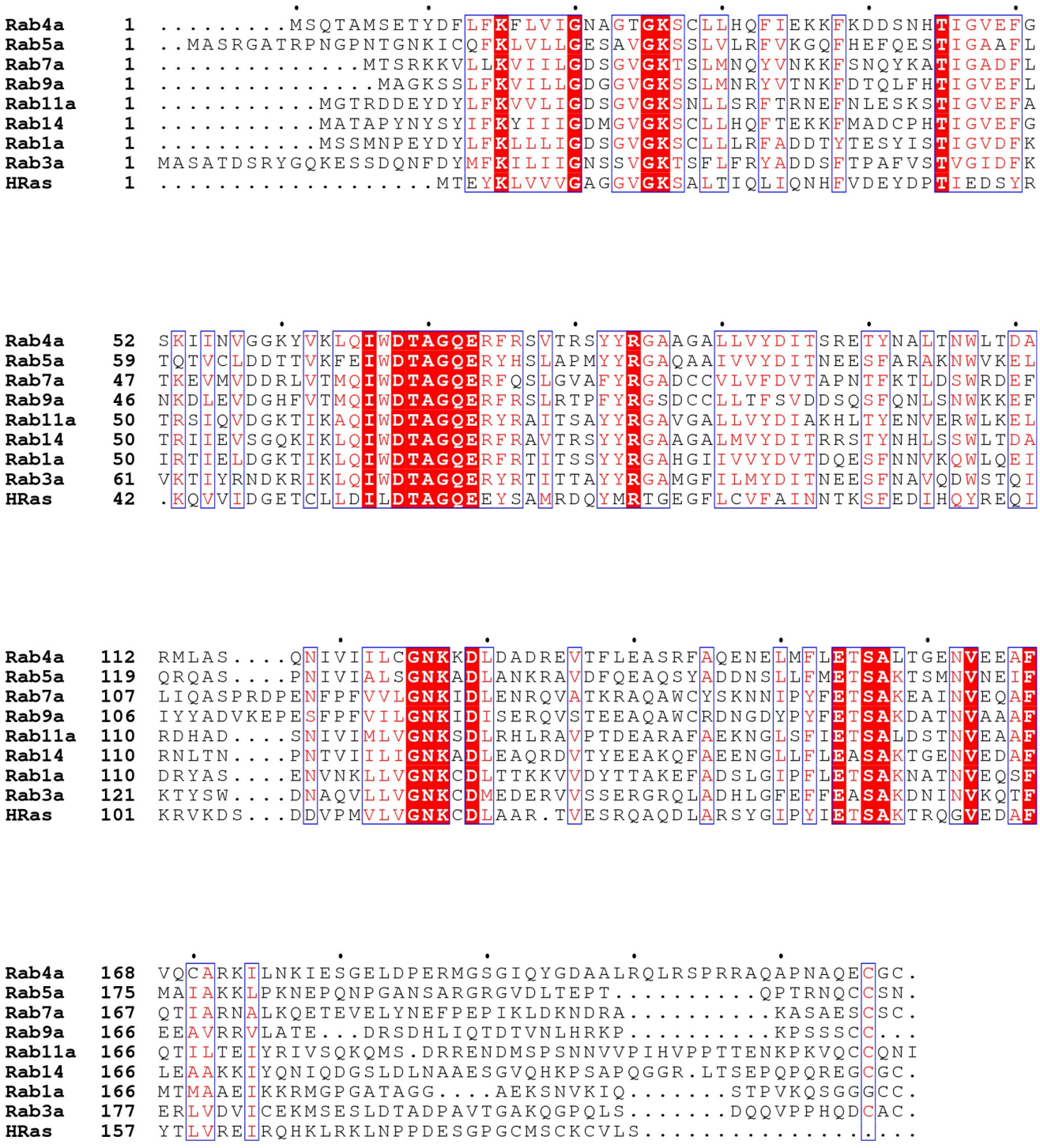

Figure 1 - figure supplement 1. Amino acid sequence alignment of the Rab- and Ras-family GTPases in human used in this study. Multiple alignment of the sequences was performed using ClustalW (http://www.genome.jp/tools/clustalw/) and ESPript 3.0 (http://espript.ibcp.fr/ESPript/ESPript/).

Figure 2. Inoshita & Mima

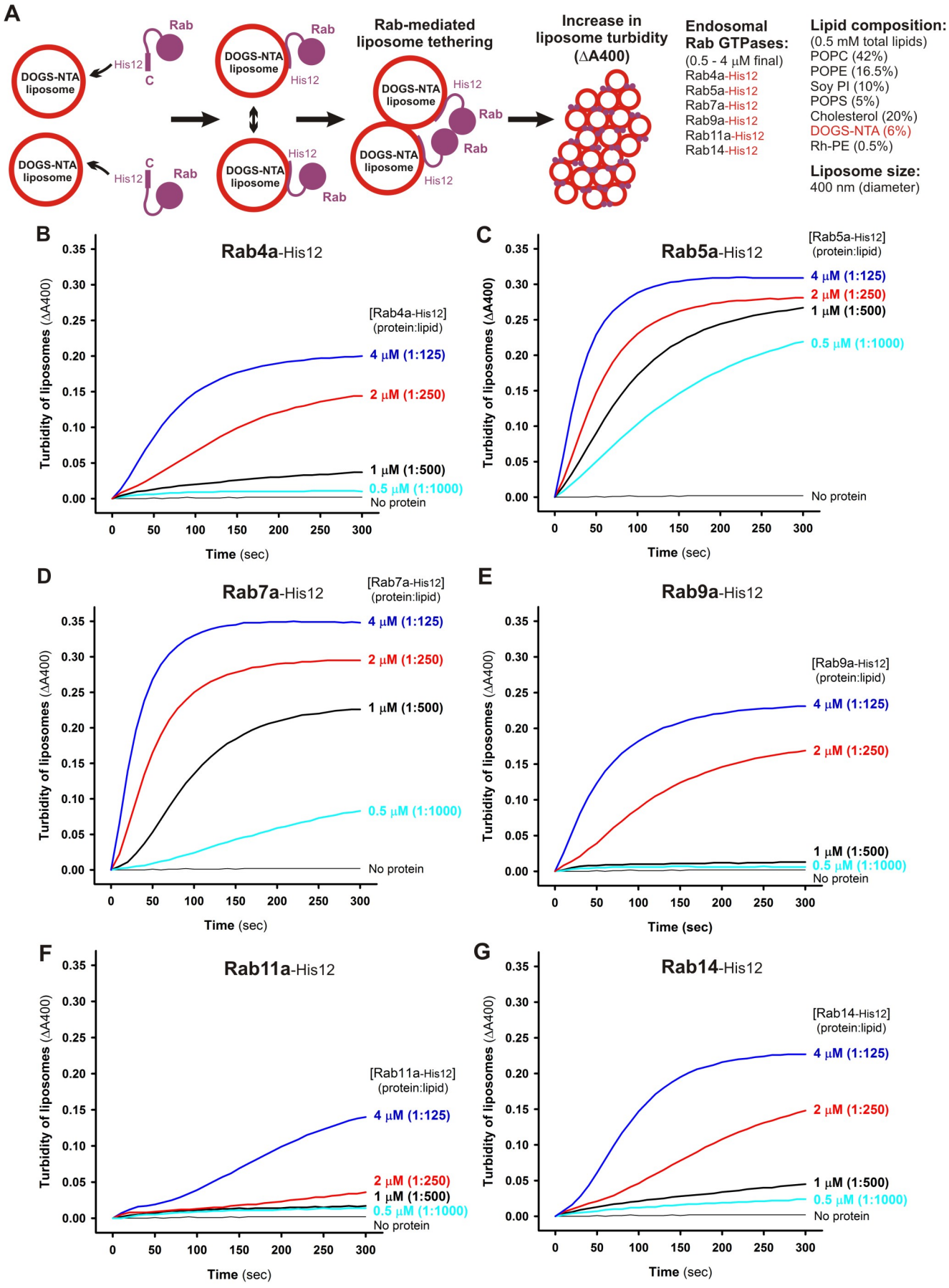

Figure 2 .Endosomal Rab GTPases directly initiate membrane tethering by themselves in a chemically defined reconstitution system.

（A) Schematic representation of liposome turbidity assays for testing Rab-mediated liposome tethering in B-G.

（B-G) Endosomal Rab-His12 proteins (0.5 - 4 μM each), Rab4a-His12 (B), Rab5a-His12 (C), Rab7a-His12 (D), Rab9a-His12 (E), Rab11a-His12 (F), and Rab14-His12 (G), were incubated with synthetic liposomes bearing physiological mimic lipid composition (400 nm diameter; 0.5 mM lipids) in RB150 containing MgCl2 (5 mM) and DTT (1 mM) at room temperature for 300 sec. During incubation, turbidity changes of the Rab-liposome mixed reactions were monitored by measuring the absorbance at 400 nm. The protein-to-lipid molar ratios used for these turbidity reactions were from 1:1000 to 1:125, as indicated.

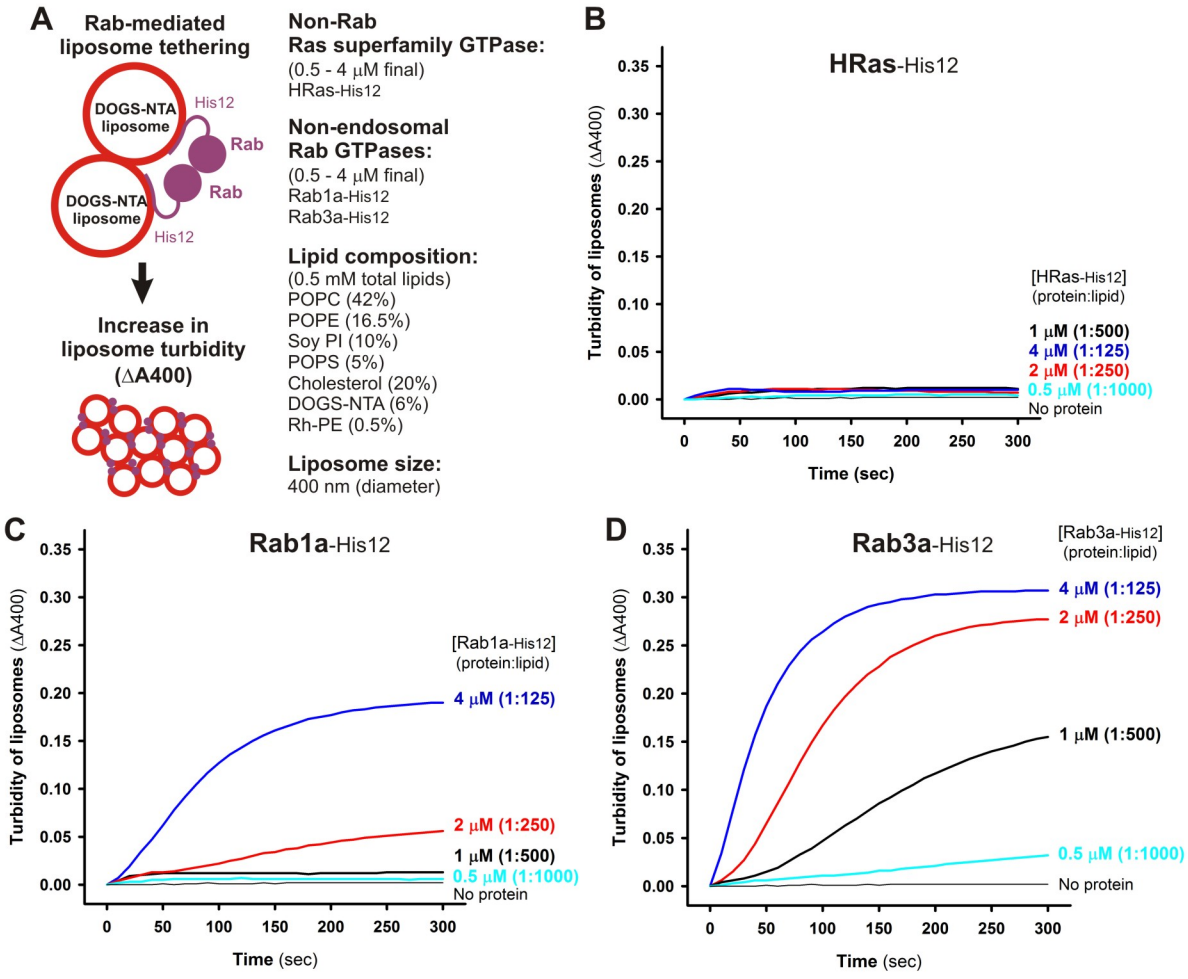

Figure 3. Non-endosomal Rab GTPases have the inherent potency to specifically mediate membrane tethering.

（A) Schematic representation of liposome turbidity assays for the non-Rab Ras superfamily GTPase, HRas, and non-endosomal Rab GTPases, Rab1a in ER-Golgi traffic and Rab3a in exocytosis, in B-D.

（B-D) Liposome turbidity assays were employed as in Figure 2B-G, with HRas-His12 (B), Rab1a-His12 (C), and Rab3a-His12 (D) proteins (0.5 - 4 μM each in final) and physiological mimic synthetic liposomes (0.5 mM total lipids in final). The protein-to-lipid molar ratios used were indicated.

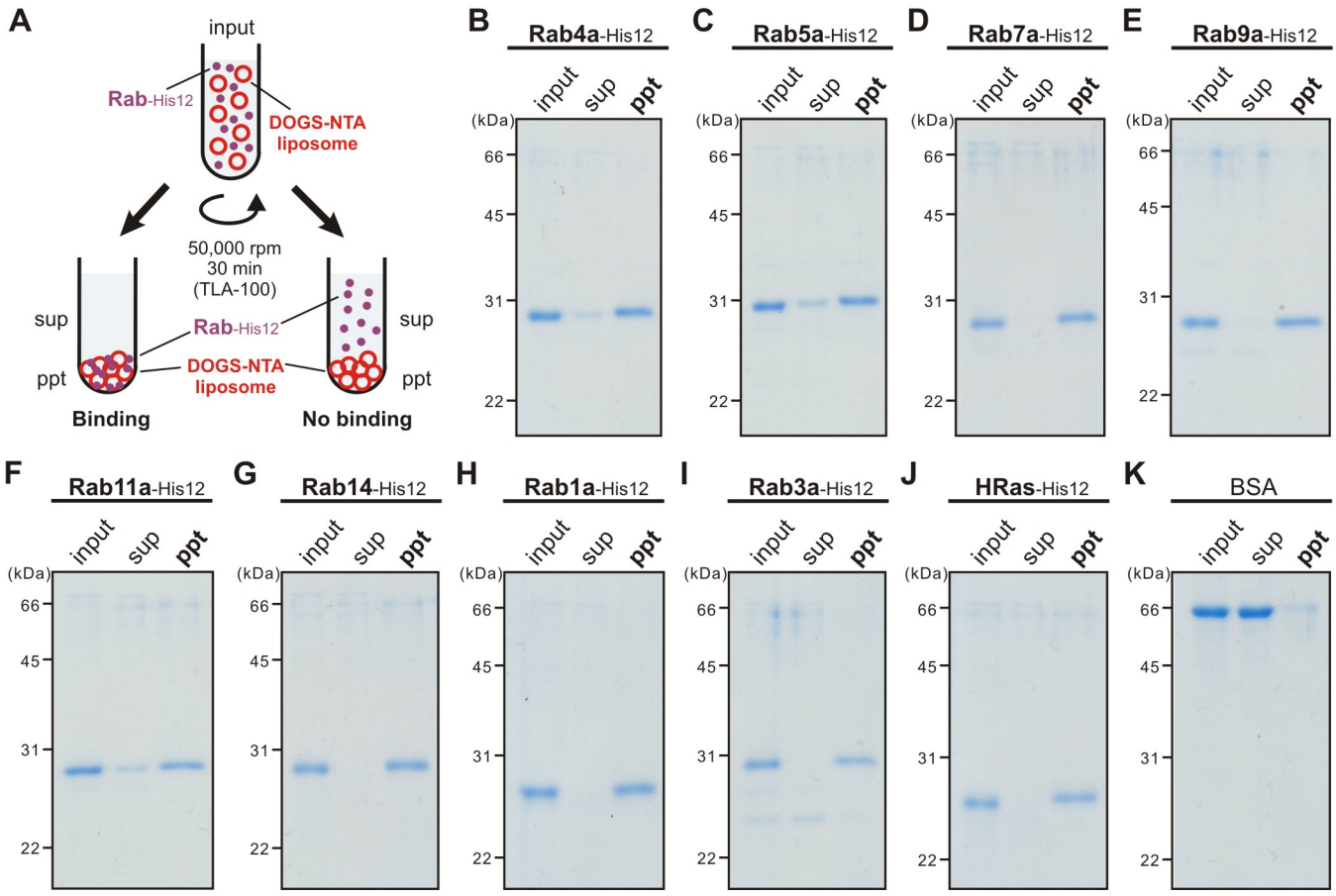

Figure 4. Membrane association of Rab-His12 proteins onto DOGS-NTA-bearing liposomes.

(A) Schematic representation of liposome co-sedimentation assays for testing membrane attachment of Rab-His12 proteins used in Figures 2-3.

(B-K) Rh-labeled liposomes (400 nm diameter; 1 mM total lipids in final) were incubated (30°C, 30 min) with Rab4a-His12 (B), Rab5a-His12 (C), Rab7a-His12 (D), Rab9a-His12(E), Rab11a-His12 (F), Rab14-His12 (G), Rab1a-His12 (H), Rab3a-His12 (I), HRas-His12 (J), and BSA for a negative control (K) (2 μM final for each), and ultracentrifuged (50,000 rpm, 30 min, 4°C). The supernatants (sup) and precipitates (ppt) obtained were analyzed by SDS-PAGE and Coomassie Blue staining.

Figure 5. Inoshita & Mima

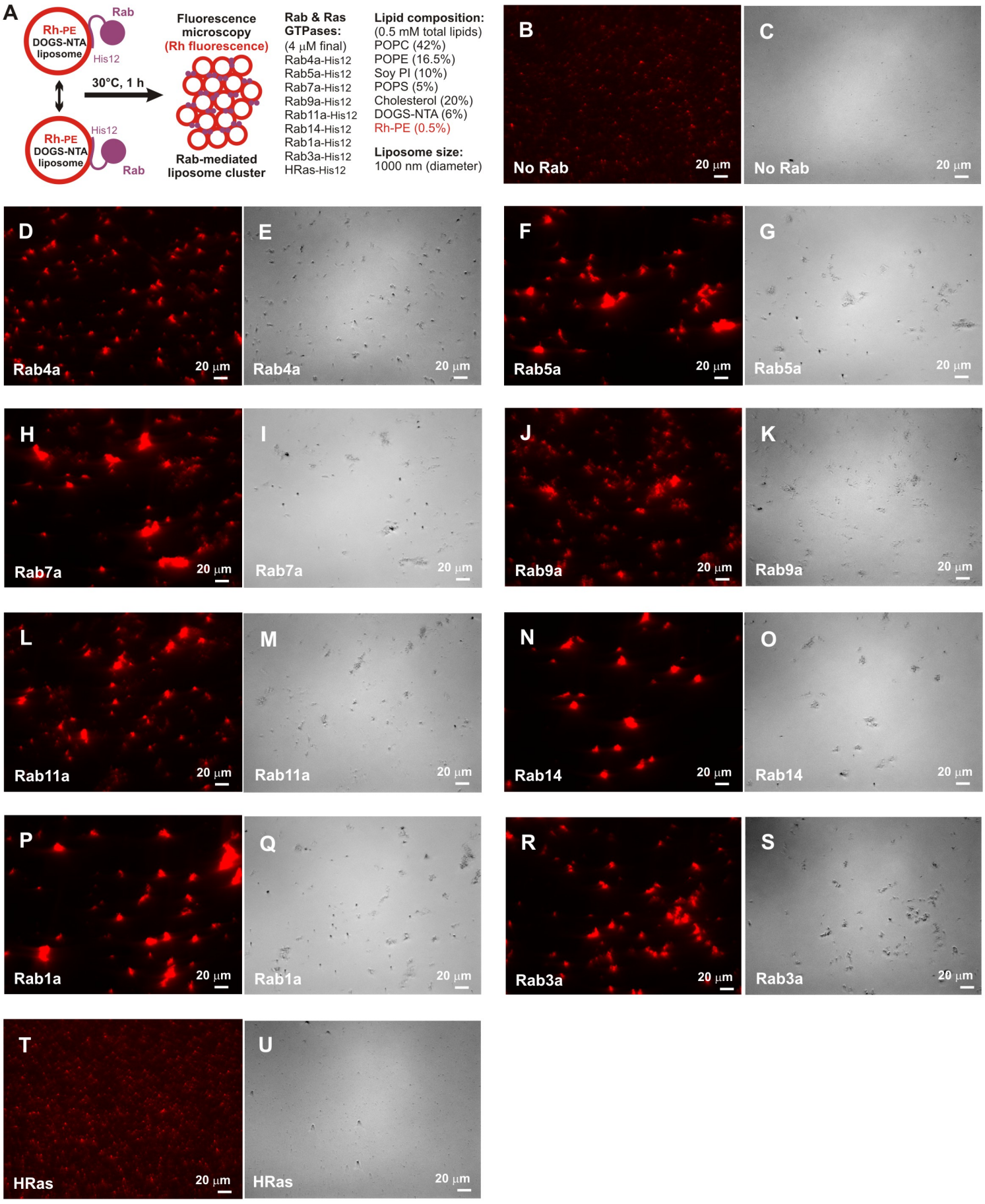

Figure 5. Rab-mediated membrane tethering induces the formation of massive liposome clusters.
（A) Schematic representation of fluorescence microscopic observations of Rab-mediated liposome clusters.
（B-U) Fluorescence images (B, D, F, H, J, L, N, P, R, T) and bright field images (C, E, G, I, K, M, O, Q, S, U) of Rab-mediated liposome clusters. Fluorescently-labeled liposomes bearing Rh-PE (1000 nm diameter; 0.5 mM lipids in final) were incubatedat 30°C for 1 h, in the absence (B, C) and presence of the Rab- and Ras-family GTPases (4 μM each in final), including Rab4a-His12 (D, E), Rab5a-His12 (F, G), Rab7a-His12 (H, I), Rab9a-His12 (J, K), Rab11a-His12 (L, M), Rab14-His12 (N, O), Rab1a-His12 (P, Q), Rab3a-His12 (R, S), and HRas-His12 (T, U),and subjected to fluorescence microscopy. Scale bars: 20 μm.

A

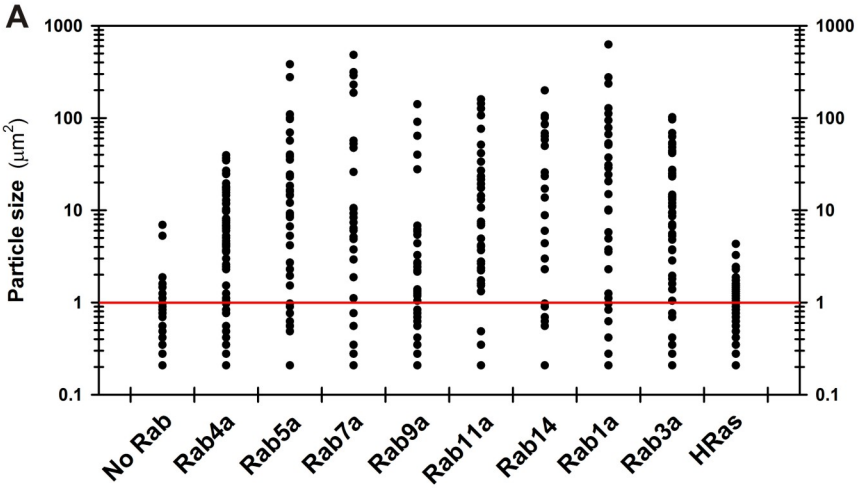

B

Rab protein	Particle number	Average size (μm²)
No Rab	38	0.92
Rab4a-His12	67	7.8
Rab5a-His12	45	32
Rab7a-His12	33	53
Rab9a-His12	55	7.9
Rab11a-His12	35	27
Rab14-His12	25	37
Rab1a-His12	36	55
Rab3a-His12	51	18
HRas-His12	96	0.80

Figure 6. Particle size distributions of liposome clusters induced by Rab-mediated membrane tethering.
（A) Particle sizes of the Rab-mediated liposome clusters observed in the fluorescence images of Figure 5.
（B) Particle numbers and average sizes of the Rab-mediated liposome clusters observed in the fluorescence images of Figure 5.

Figure 7. Inoshita & Mima

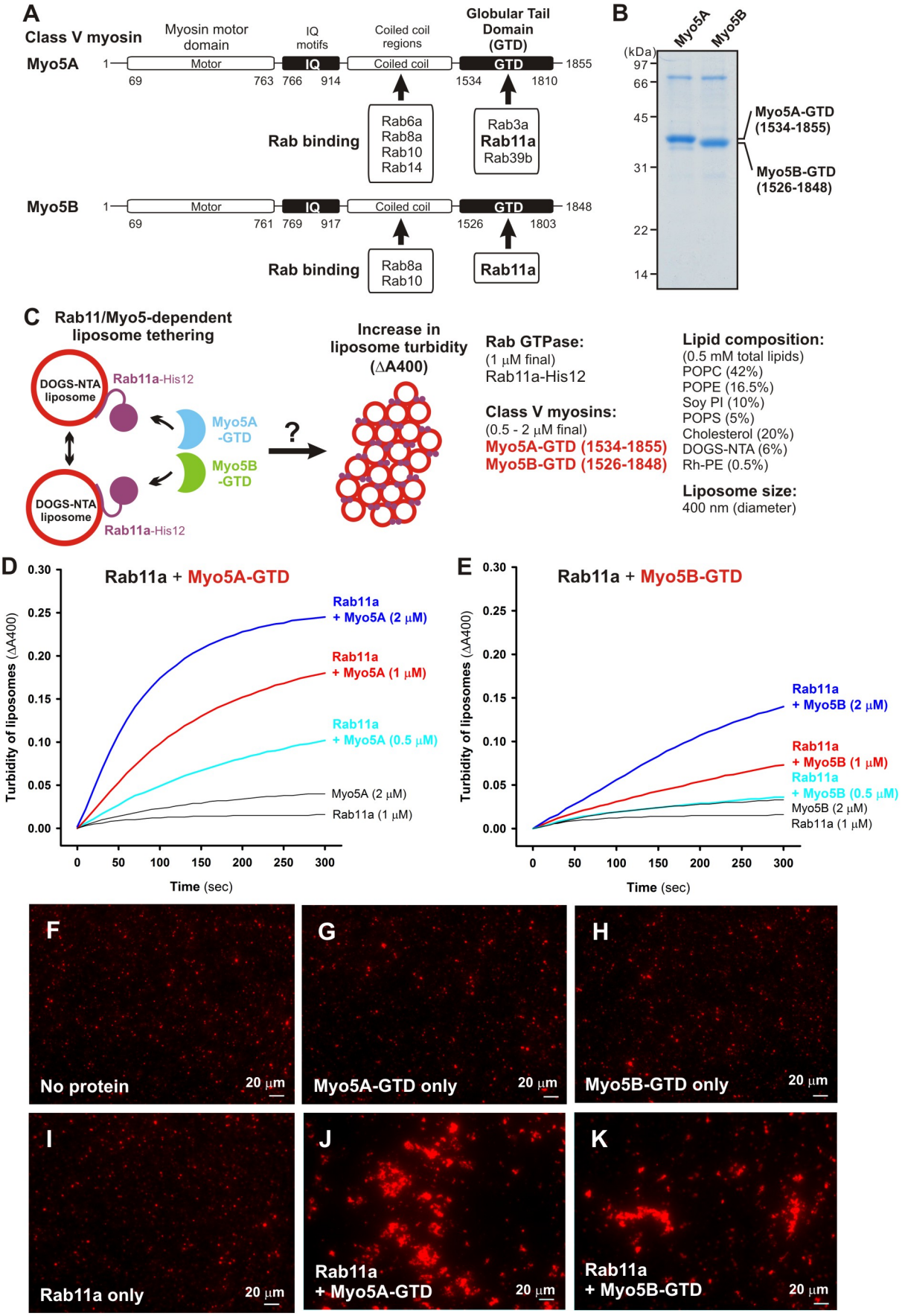

Figure 7. Class V myosin globular tail domains, Myo5A-GTD and Myo5B-GTD, strongly stimulate Rab11a-dependent membrane tethering.

（A) Schematic representation of class V myosins in human, Myo5A and Myo5B, showing their amino acid residuesand domains including myosin motor domains, IQ motifs, coiled coil regions, and globular tail domains (GTDs).Representative Myo5-interacting Rab GTPases and the Rab-binding regions in Myo5A and Myo5B are indicated.

（B) The Coomassie Blue-stained gel of purified Myo5A-GTD and Myo5B-GTD proteins, which are comprised of the amino acid residues 1534-1855 and 1526-1848, respectively.

（C) Schematic representation of liposome turbidity assays for testing Rab11a- and Myo5-GTD-dependent liposome tethering in D, E.

（D,E) Liposome turbidity assays were employed with Rab11a-His12 (1 μM final) as in Figure 2F, but in the presence of Myo5A-GTD (D) and Myo5B-GTD (E) (0.5 - 2 μM final).

（F-K) Fluorescence images of Rab11a-mediated liposome clusters in the presence of Myo5-GTDs. Rab11a-His12 (3 μM final) and Myo5A-GTD or Myo5B-GTD (3 μM final) were preincubated at 30°C for 30 min, mixed with Rh-labeled liposomes (1000 nm diameter; 0.8 mM lipids in final), further incubated (30°C, 30 min), and subjected to fluorescence microscopy (J, K). For a control, Rab11a-His12, Myo5-GTD, or both were omitted from the reactions where indicated (F-I). Scale bars: 20 μm.

Figure 8. Inoshita & Mima

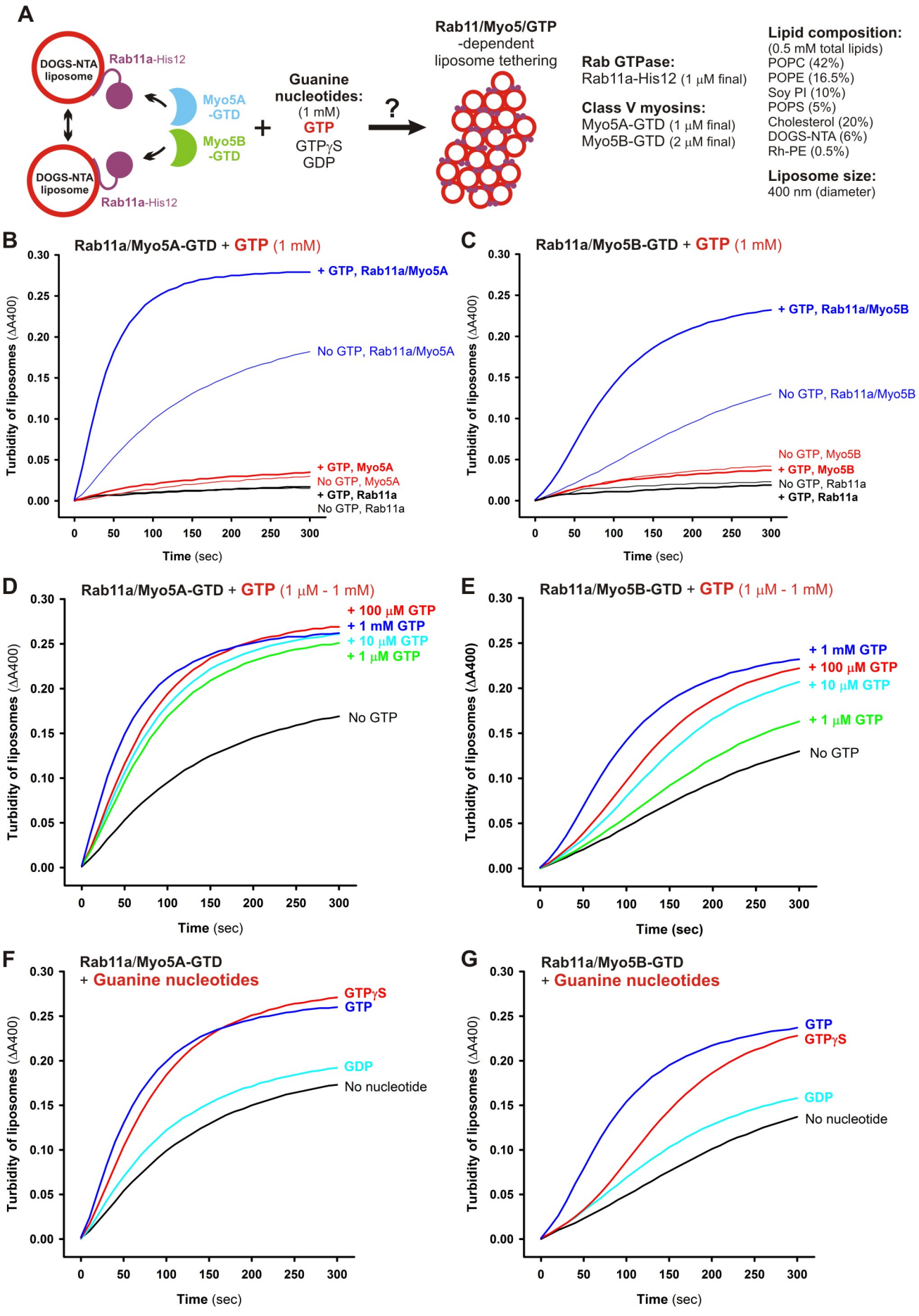

Figure 8. Guanine nucleotide dependence of Rab11a-mediated membrane tethering in the presence of Myo5A-GTD and Myo5B-GTD.

（A) Schematic representation of liposome turbidity assays for testing Rab11a- and Myo5-GTD-dependent liposome tethering in the presence of GTP in B-G.

（B, C) Rab11a/Myo5-dependent membrane tethering is strongly and specifically promoted by the addition of GTP. Liposome turbidity assays with Rab11a-His12 (1 μM) and Myo5A-GTD (1 μM) (B) or Myo5B-GTD (2 μM) (C) were performed as in Figure 7D, E, but in the presence of GTP (1 mM).

（D, E) Liposome turbidity assays were employed with Rab11a-His12 and Myo5A-GTD (D) or Myo5B-GTD (E) as in B, C, in the presence of various concentrations of GTP (1 μM - 1 mM).

（F, G) Liposome turbidity assays were employed with Rab11a-His12 and Myo5A-GTD (F) or Myo5B-GTD (G) as in B, C, in the presence of GTP, GTPγS, and GDP (1 mM for each).

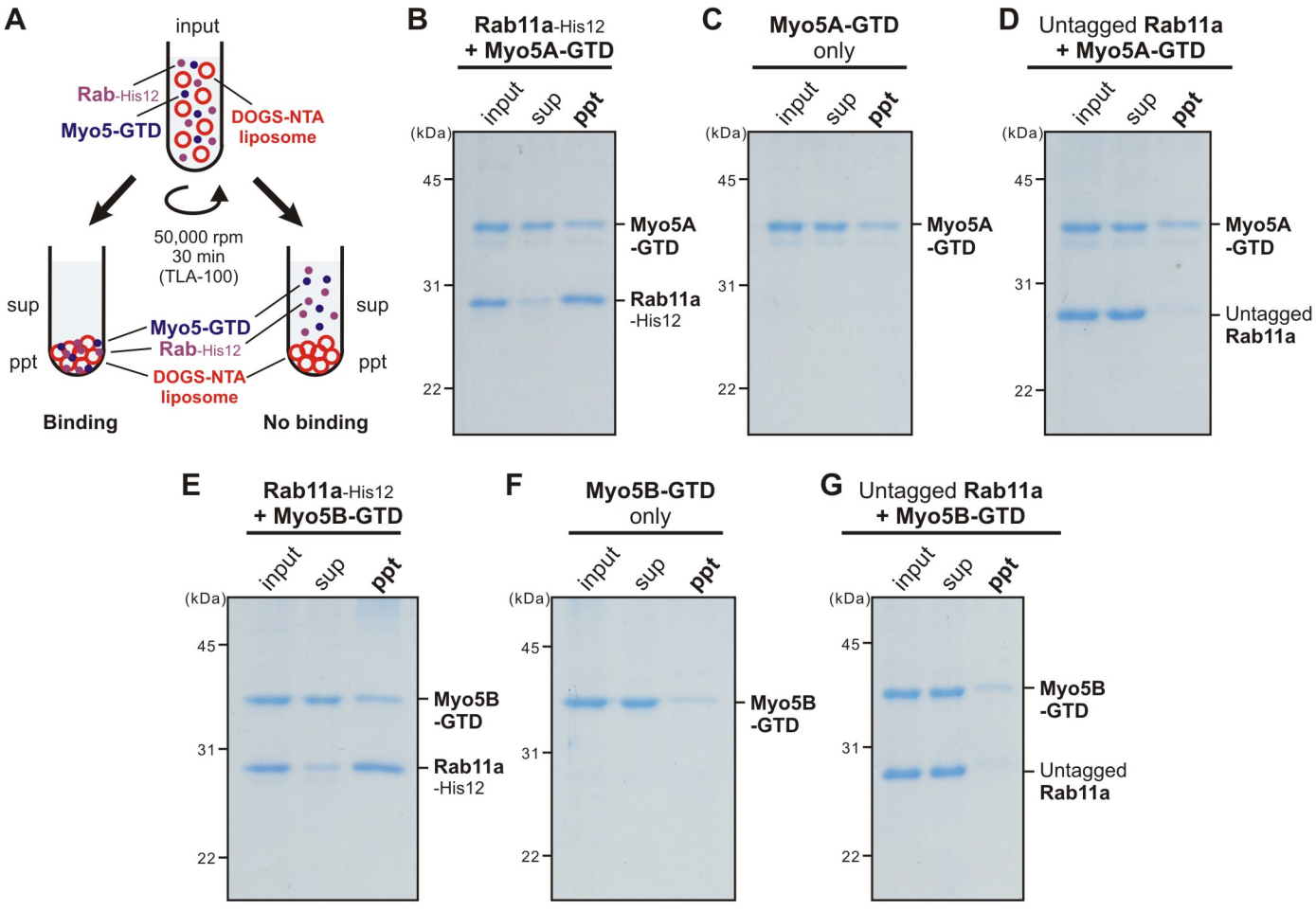

Figure 9. Membrane association of Myo5-GTD proteins onto Rab11a-anchored liposomes.

（A) Schematic representation of liposome co-sedimentation assays for testing membrane binding of Myo5A-GTD and Myo5B-GTD to Rab11a-bound liposomes.

（B-G) Liposome co-sedimentation assays were employed as in Figure 4, with Rh-labeled liposomes (400 nm diameter; 1 mM lipids) and Rab11a-His12 (2 μM) (B, E), but in the presence of Myo5A-GTD (2 μM) (B-D), Myo5B-GTD (2 μM) (E-G), and GTP (1 mM). For a control, the reactions without Rab11a-His12 (C, F) or with the untagged form of Rab11a lacking a His12 tag (untagged Rab11a) (D, G) were also tested. The supernatants (sup) and precipitates (ppt) obtained were analyzed by SDS-PAGE and Coomassie Blue staining.

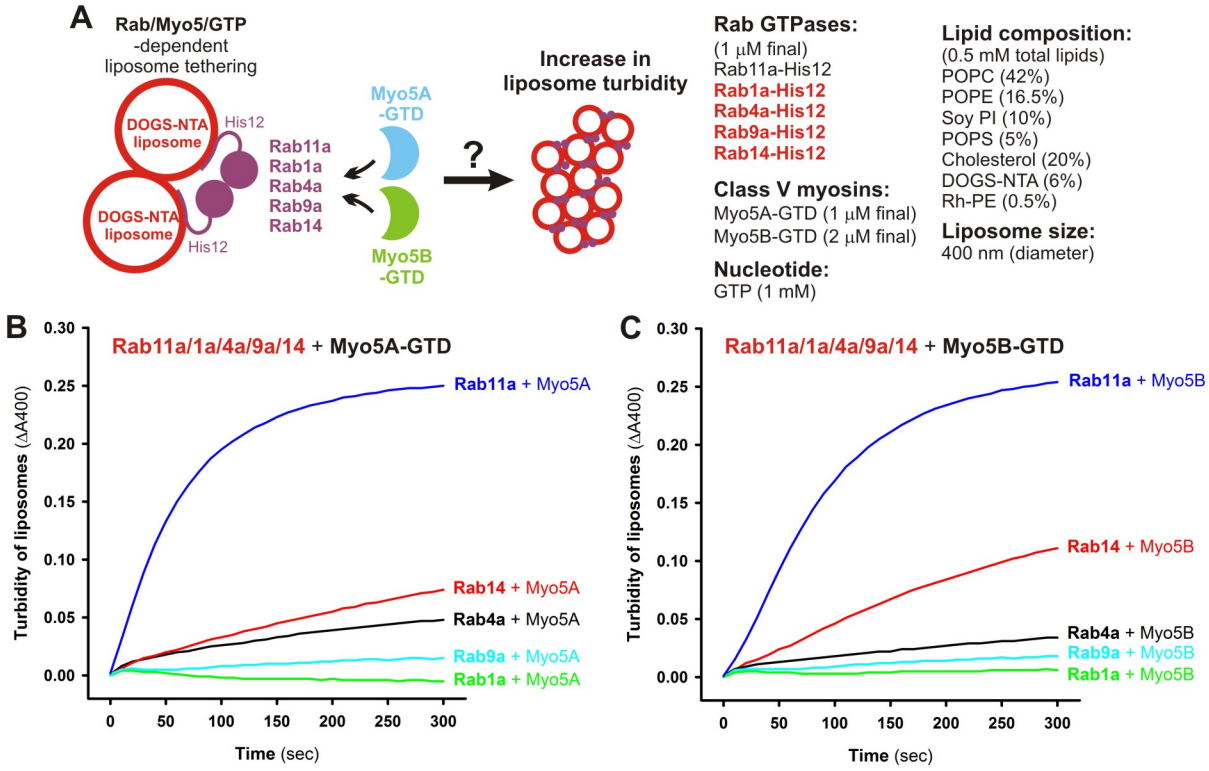

Figure 10. Myo5A-GTD and Myo5B-GTD selectively activate Rab11a-dependent membrane tethering.
(A) Schematic representation of liposome turbidity assays in B, C, for the various Rab GTPases (Rab11a, Rab1a, Rab4a, Rab9a, Rab14) in the presence of Myo5-GTDs and GTP.
(B, C) Myo5-GTDs specifically promote efficient membrane tethering mediated by the cognate Rab GTPase, Rab11a. Liposome turbidity assays were employed with Myo5A-GTD (B) or Myo5B-GTD (C) and GTP, as in Figure 8B, C, but for Rab11a, Rab1a, Rab4a, Rab9a, and Rab14 GTPases.